ABSTRACT

A SEARCH FOR STAR-PLANET MAGNETIC INTERACTION USING TIME-RESOLVED DIFFERENTIAL PHOTOMETRY THROUGH A CA K FILTER

This thesis presents an innovative approach to detecting star-planet magnetic interaction (SPMI) through the exploration of magnetic variability in stellar light curves. We employed the use of a Calcium K-line (Ca K) filter to obtain time-resolved differential photometry of selected variable stars. The gathered data were then analyzed to detect any variability, and also used to calculate Lomb-Scargle periodograms, to detect periodicity in the variability. Our methodology allowed for the detection of potential magnetic interaction between stars and their associated planets, a phenomenon that could uniquely provide information about exoplanet interiors. By bridging photometry and magnetic field studies, this research contributes to our understanding of stellar activity and its impact on exoplanetary environments. The findings from this study pave the way for further investigations into the multifaceted star-planet interactions and their implications for exoplanet habitability and star-planet co-evolution.

Sourav Kharat
December 2023

A SEARCH FOR STAR-PLANET MAGNETIC INTERACTION WITH TIME-RESOLVED DIFFERENTIAL PHOTOMETRY THROUGH A CA K FILTER

by

Sourav Kharat

A thesis

submitted in partial

fulfillment of the requirements for the degree of

Master of Science in Physics

in the College of Science and Mathematics

California State University, Fresno

December 2023

Note: Do not use academic titles (i.e., Dr., Ph.D.) when you enter your committee members' names on this page. Use first and last name only. When filling in the department name, do not use "Department of…" Simply use Biology or English or Psychology.

APPROVED

For the Department of Physics:

We, the undersigned, certify that the thesis of the following student meets the required standards of scholarship, format, and style of the university and the student's graduate degree program for the awarding of the master's degree.

Sourav Kharat
Thesis Author

Frederick A. Ringwald
Chairperson's name (Chair) Physics

Gerardo Muñoz
Committee member's name Physics

Ettore Vitali
Committee member's name Physics
or professional affiliation

For the University Graduate Committee:

Dean, Division of Graduate Studies

AUTHORIZATION FOR REPRODUCTION

OF MASTER'S THESIS

X I grant permission for the reproduction of this thesis in part or in its entirety without further authorization from me, on the condition that the person or agency requesting reproduction absorbs the cost and provides proper acknowledgment of authorship.

_____ Permission to reproduce this thesis in part or in its entirety must be obtained from me.

Signature of thesis author: S.Kharat

ACKNOWLEDGMENTS

I would like to thank the immense support from my mother (Vaishali Kharat) and my father (Suresh Kharat) and all my family members and friends back in India. I would like to thank Dr. Frederick Ringwald for his support and mentoring throughout my Master's Program, Dr. Gerardo Muñoz for guiding me for these two years, Dr. Ettore Vitali for being an amazing professor, Dr. Douglas Singleton for being the best department chair and all other professors I've met during my time here.

This research used photometry taken at Fresno State's station at Sierra Remote Observatories. Many thanks are extended to Dr. Greg Morgan, Dr. Melvin Helm, Dr. Keith Quattrocchi, and the other SRO observers for creating this fine facility, as well as the Department of Physics at Fresno State for supporting it. The Teaching Assistant position granted to me by the Department of Physics has been pivotal in my success. I have been awarded the Cheunjit Katkanant Memorial Scholarship by the Department of Physics in Fall 2022 and I have received several Fee Waivers because of my Teaching Assistant position, which have I have immensely appreciated.

TABLE OF CONTENTS

Page

Page

Note: The Table of Contents, List of Tables, and List of Figures are automatic. There is no need to type anything into them. When you have finished adding all text to the template, simply single-click in the Table of Contents to select it, then right-click to open the menu options. Select the option "Update Field" and fill in the circle "Update Entire Table," then click "OK." If you have applied the appropriate style (e.g., 1st-Level Centered Hdg) to your headings in the text, headings and page numbers will update in the TOC without you having to do anything. Delete this text box when you are finished.

LIST OF FIGURES

Page

Page

Page

Page

1.INTRODUCTION

1.1 THE SUN

Let us imagine a star similar to the Sun. Let's call this star Sun 2.0. Orbiting it is a planet which is similar to our own planet Earth. Let's call this planet Earth 2.0. Now this Earth 2.0 is teeming with life just like on our planet. If one day a stellar flare occurs on Sun 2.0, which is much more intense than normal standards, it would not cause all the bushes to go into flames on Earth 2.0. It would cause the ozone layer to get depleted, which would result in all the ultraviolet rays from the Sun to reach the surface of this planet, Earth 2.0 (Bais et al. 2015). Regeneration of the ozone layer takes decades to fix (Walker 2022) which will be a huge cause of danger for all the organisms living on this planet except for the ones living in water!

The Sun fortunately will never act up like this and instantaneously cause explosions. The energy output detected from the Sun has been steady over the years. The energy output has been detected from space satellites where the Earth's atmospheric effects are negligible. The solar constant has mostly been constant (funnily) only increasing by a factor 0.2% at the peak of each 11-year solar cycle. The Sun has brightened by 40% over the 4.6 billion years since it has formed. You would think that this can cause harmful effects on the surface of the Earth but the heat trapping gases in the atmosphere have compensated for it.

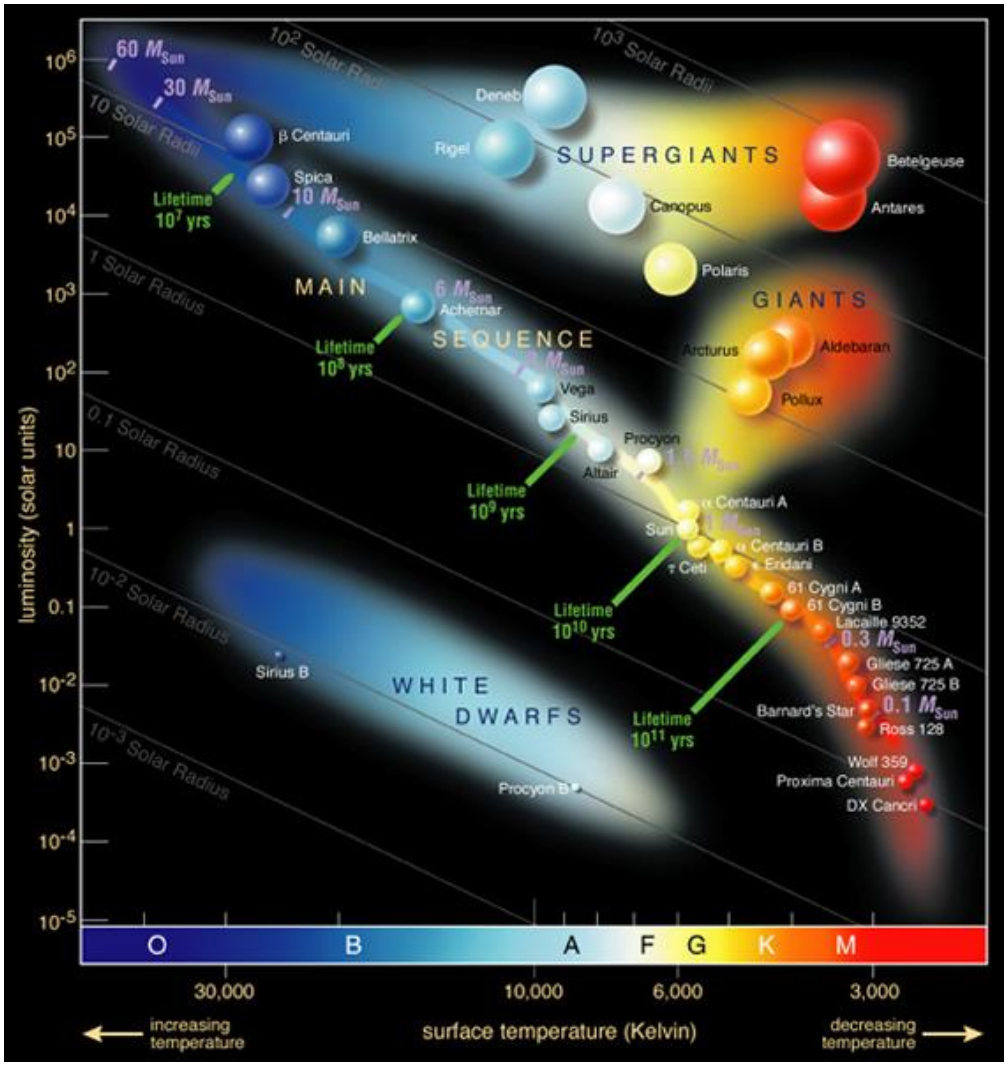

Figure 1: Hertzsprung-Russell diagram (CESAR – Cosmos 2023).

The Hertzsprung-Russell (HR) diagram is a significant tool in astrophysics. It plots stellar luminosity against surface temperature, which helps in understanding the evolutionary stages and classifications of stars (Big Think 2021; Physics LibreTexts 2023; Azo Quantum 2023). The diagram shows most stars lying on the main sequence, a trajectory extending from high temperature and high luminosity to low temperature and low luminosity, representing a phase in a star's life where hydrogen fusion occurs in the star's core (Physics LibreTexts 2023). Developed in 1910 by astronomers Ejnar

Hertzsprung and Henry Norris Russell, the HR diagram has been instrumental for stellar classification and understanding the interrelations among different types of stars (Devorkin 1978; Universe Today 2023a).

The Sun is classified as a G-type main-sequence star, often referred to as a G-type yellow-dwarf star, although it's actually yellow-white in color. This classification is rooted in the Sun's spectral characteristics and its position on the main sequence of the HR diagram, where it's in the phase of fusing hydrogen into helium in its core (Exoplanet Exploration 2021; Universe Today 2023b). The G-type classification indicates a certain temperature range, and being a main-sequence star, denotes a specific stage in the Sun's life cycle. The Sun, representing a typical G-type main-sequence star, possesses characteristics such as having about 99.86% of the mass of the Solar System and an absolute magnitude of +4.83 (Universe Today 2023b). Unlike most stars in the Universe, which are cooler and have a lower mass, the Sun's attributes place it in a stable phase of its life cycle, expected to continue for a few billion more years before transitioning to the next evolutionary stage (AstroBackyard 2020). This signifies that the Sun is quite "unremarkable" in a good sense, which has everything to do with the fact that it supports life on Earth. The Sun only has moderate levels of activity, which appear as solar flares. Earth's terrestrial magnetic field deflects the charged particles from these solar flares, the X-rays from solar flares are absorbed by the upper atmosphere, and the stratospheric ozone absorbs all the ultraviolet rays.

1.2 VARIABLE/INCONSTANT SUNS

Many stars vary over time and are not like the Sun, which is constant. These stars vary over a period of hours, days, and months. Astrophysicists classify these "variable

stars" according to their properties. They are classified as geometric variables, eruptive variables, and pulsators:

A) GEOMETRIC VARIABLE

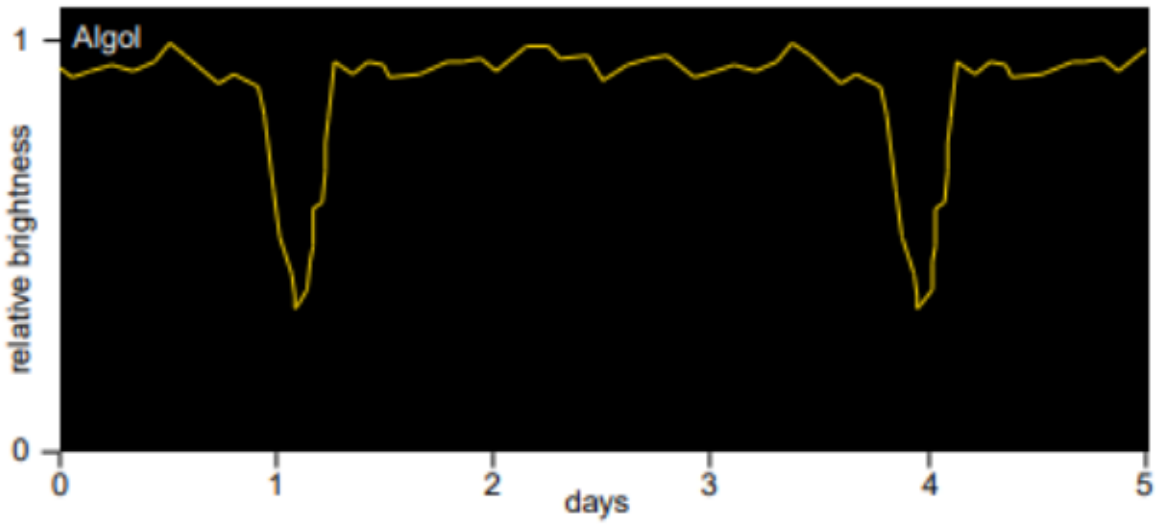

Figure 2. Magnitude of Beta Persei as a function of time (From: Rubenstein 2001).

The figure above represents the magnitude or brightness over a period of days of the star Algol (Beta Persei), which is categorized as a geometric variable. The variation in the magnitude of geometric variables is mostly caused by the viewing geometry. When another star in a binary system passes in front of the other it causes the apparent brightness of the star, which is being observed to become fainter for a short time.

B) ERUPTIVE VARIABLE

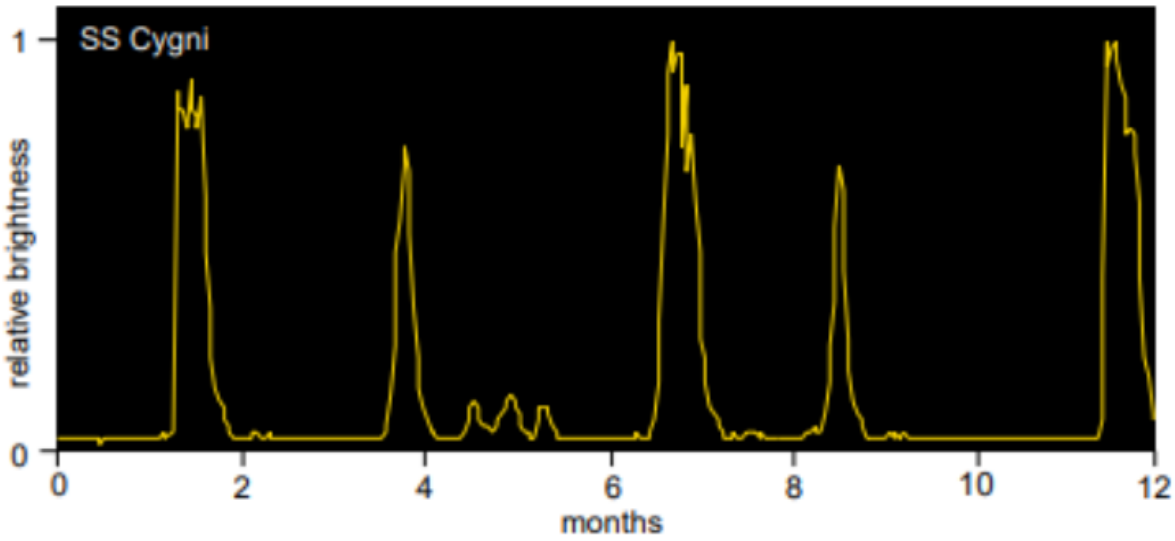

Figure 3. Magnitude of SS Cygni as a function of time (From: Rubenstein 2001)

The figure above is the relative brightness of the star SS Cygni, known as an eruptive variable. As you can see, the brightness is spiking in the graph above. It's because of the repeated outbursts and the time between successive outbursts is not steady. Eruptive variables consist of supernova stars that end their lives by exploding violently, as well as cataclysmic variables, which is a type of a binary star system consisting of a red dwarf accretion onto a white dwarf. SS Cygni is the brightest known dwarf nova, a subclass of the cataclysmic variables (Giovanelli & Martinez-Pais 1991; Bitner et al. 2007; Miller-Jones et al. 2013).

C) PULSATING VARIABLE

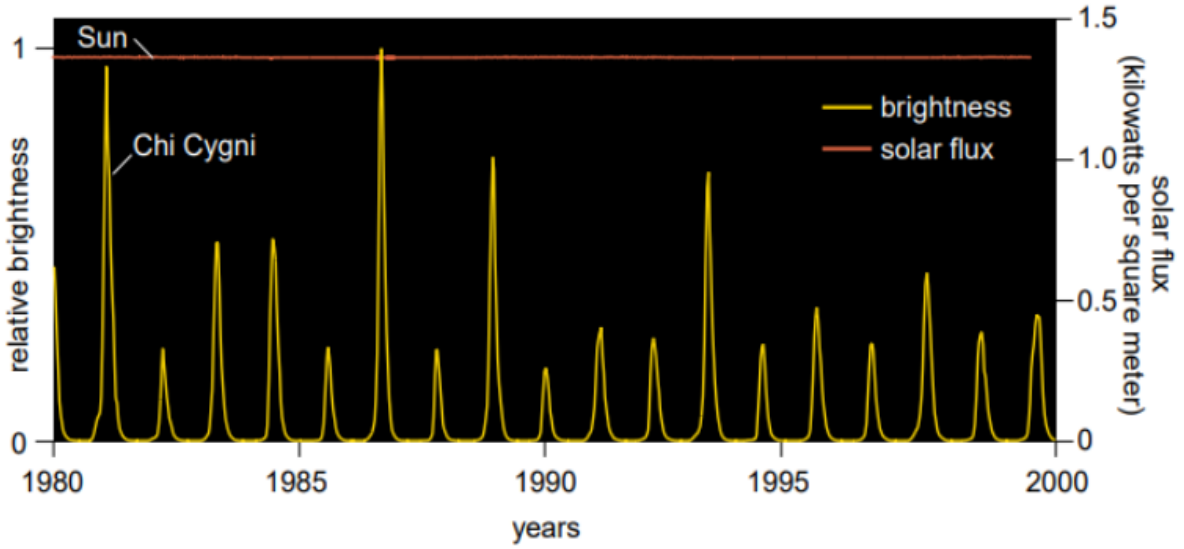

Figure 4. Magnitude of Chi Cygni as a function of time (From: Rubenstein 2001)

Another type of variables observed are the pulsators, or the pulsating variables. The graph shown above is of a pulsator star Chi Cygni. These variables vary mostly periodically but some have multiple periodicities superimposed.

1.3 SOLAR ANALOGUES

As discussed in the previous section, we quickly find out that not all stars are like the Sun. The Sun, being quite steady and unremarkable, supports life but most of the other stars are variable. More than 100,000 stars have been observed to be variable and been cataloged.

Chromospheric activity in stars signifies magnetic phenomena in their outer atmosphere, showcased by strong absorption lines such as the H and K lines of singly ionized calcium. These Ca II H and K lines are tightly connected to the stellar surface magnetic fields, illuminating the interaction between magnetic fields and atmospheric conditions (Dineva et al. 2022). If we started looking at stars that are comparable to the Sun in size, radius, and chromospheric activity, this could lead to us finding planets that are habitable like our Earth. Such stars are called *Solar Analogues*.

1.4 NOT SO SUN-LIKE

Many instances of such Sunlike stars have been studied, and astrophysicists have found out that nine of these stars have superflares, having energies in the order of 10^{35} to 10^{38} ergs, where 1 erg = 10^{-7} Joules. Normal solar flares have energies to 10^{29} to 10^{31} ergs. The harmful radiation splurging out of these superflares would not be supportive for a habitable planet orbiting it. Schaefer et al. (2000) found that:

1) They are not closely spaced binary stars, which might cause tidal interactions on their chromosphere that would increase their magnetic fields, causing superflares.
2) They are not young stars, which means they are not rotating rapidly.

3) They are not rotating rapidly, which might cause a boost in the chromospheric activity leading to super flares.

So, the mystery was, what was causing these superflares?

1.5 MAGNETIC RECONNECTION

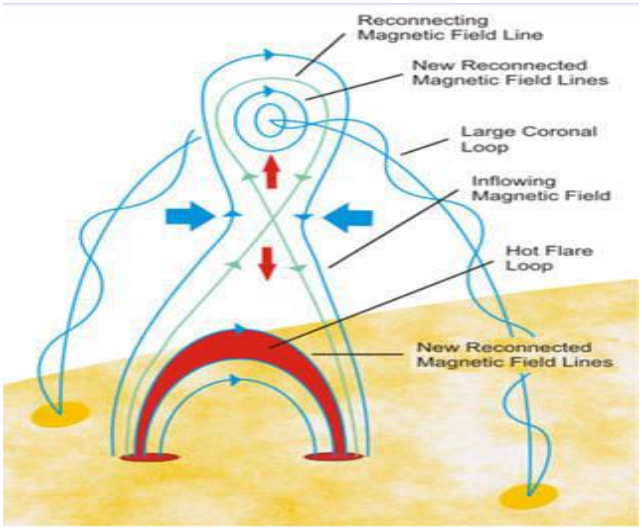

Figure 5: Illustration of Magnetic Reconnection in a solar flare (From: Public-domain image from NASA)

Magnetic reconnection is the phenomenon where magnetic field lines get entangled and reconnect. Just like one can imagine rubber bands getting entangled and breaking, magnetic field lines have the ability to stretch and break. (Dungey 1961; for reviews, see Priest & Forbes 2000 and Hesse & Casssak 2019).

For decades, magnetic reconnection was suspected to be the reason behind solar flares (Giovanelli 1948; Hoyle 1949; Dungey 1953). Finally in 2012, with the High-Resolution Coronal Imager telescope on a sub-orbital rocket, magnetic reconnection in solar flares was observed (Cirtain et al. 2013).

1.6 STAR-PLANET MAGNETIC INTERATION

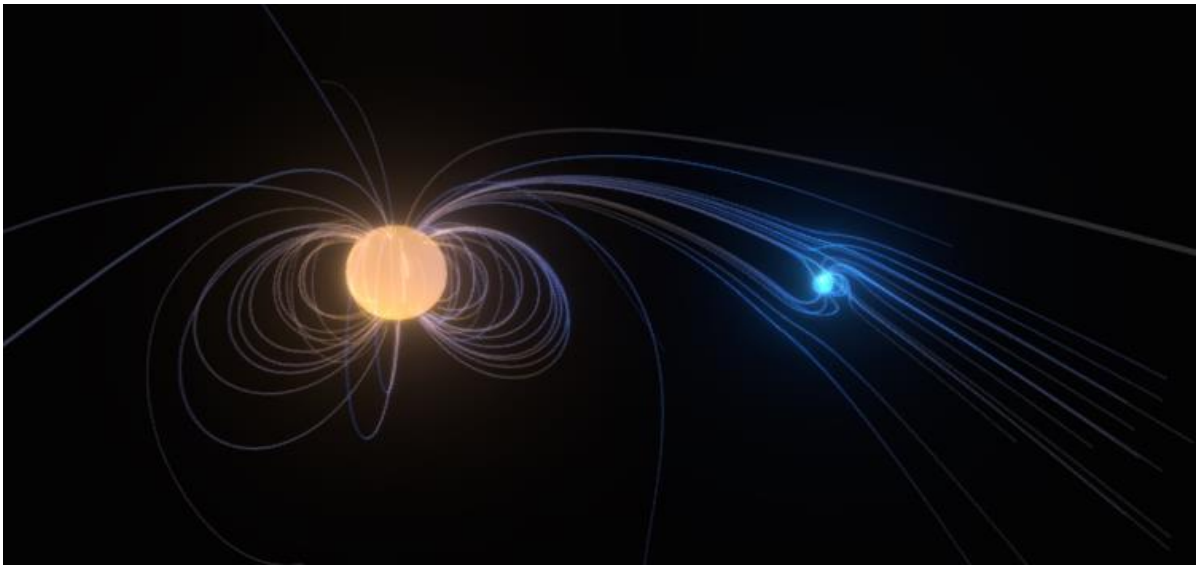

Figure 6: A 3-d model of Star Planet Magnetic Interaction. (From: Pillitteri, (2019). Star planet magnetic interaction. Retrieved from https://sketchfab.com/3d-models/star-planet-magnetic-interaction-71a173d76fc6419a8965ba2580784a27)

Star-planet magnetic interaction (SPMI) represents a theorized form of activity that could take place when a planet is in such proximity to its host star that their respective magnetic fields intertwine. In the Solar System in which we live, magnetic interactions between planets and their surroundings are recognized to result in phenomena such as auroras. The discovery of numerous exoplanets in close orbits around their host stars has encouraged interest in understanding the magnetic dynamics in different star-planet systems. This has led to the revelation of multiple magnetic effects, including potential planet inflation or heating, planet migration, the escape of planetary matter, and even alterations in the observable activity of the host star (Strugarek 2021).

1.7 COST OF DETECTING STAR PLANET MAGNETIC INTERACTION

Evgenya Shkolnik's pivotal work in discerning star-planet magnetic interactions (SPMIs) notably utilized the Canada-France-Hawaii Telescope (CFHT) and its high-resolution Gecko spectrograph, focusing on the Ca II H and K emission lines within high-resolution spectra to unveil magnetic interactions between celestial bodies (Shkolnik et al. 2003; Shkolnik et al. 2005, Shkolnik et al. 2008). Constructed in 1979, the CFHT, with its 3.58-meter aperture, represented a substantial investment of around $20 million, aligning with the typical financial framework for 4-meter-class telescopes (Kitchin 2021). The employment of Gecko, a coude'-echelle spectrograph, was crucial for extracting detailed spectral data, albeit with costs exceeding $1 million (Kitchin 2021). This financial commitment underscores the significant funding essential for advancing astronomical research and understanding, particularly in exploring the magnetic dynamics within star-planet systems.

For this thesis, we are using data from Fresno State's Sierra Remote Observatories, which cost around $120,000, a small fraction of the amount of money usually spent to detect SPMI. The aim of this thesis is to create a new methodology using budget-friendly equipment to detect SPMI.

2.METHODOLOGY

In our method, we will be utilizing astronomical pictures of fields which have the stars (suspected to have exoplanets or SPMI) taken through the Sierra Remote Observatory. We will then subject the raw data to time resolved differential photometry. Using this resultant time resolved differential photometry data, we will perform various analysis techniques on this data. Our aim is to find periodicity in this data which will indicate magnetic variability.

2.1 SIERRA REMOTE OBSERVATORIES

The Sierra Remote Observatories (SRO) provide hosting services for remotely operated telescopes situated in the Sierra Nevada Mountains, near Shaver Lake at an altitude of 4610' (1405 m). Established in 2007, SRO hosts over 125 telescope systems as of the latest data. The observatories were initiated by Dr. Greg Morgan, Dr. Keith Quattrocchi, and Dr. Mel Helm, who are members of the Central Valley Astronomers. Fresno State's telescope is housed in Observatory #7. This setup enables various stakeholders, including astrophotographers, other universities, professional research observatories, NASA, and commercial satellite tracking companies (Sierra Remote Observatories 2023).

2.2 TIME-RESOLVED PHOTOMETRY

For the time-resolved photometry method, we are using The Handbook of Astronomical Image Processing Software (Berry & Burnell 2000). We first need to take a bunch of different images of a variable star's field, for which we wish to obtain its light curve.

Calibrations include dark frames, raw flat fields, and flat darks. We use the dark frames and median combine them to make the master dark. We use the raw flat fields and flat darks to make the master flat. This process is shown in a representation below:

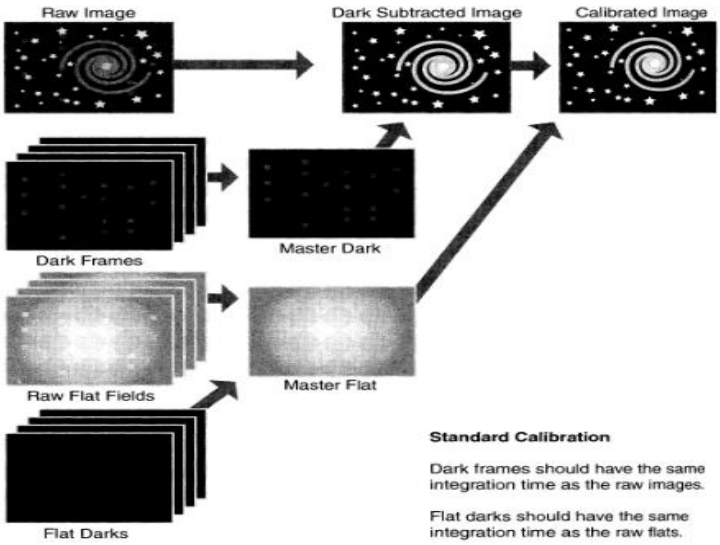

Figure 7: Representation of advanced calibration of deep-sky images for time-resolved photometry (From: Berry & Burnell 2000)

We follow the prompts in the software to produce a calibrated deep sky image containing our variable star.

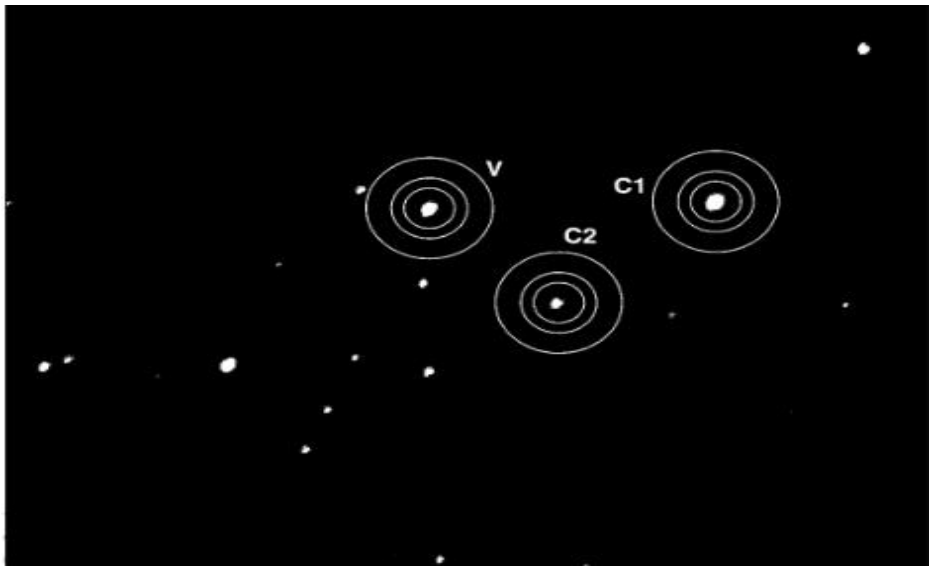

Figure 8: V is the variable star, C1 is the comparison star, C2 is the check star (From: Berry & Burnell 2000)

Now, we need to choose a variable star, a check star and a comparison star. After choosing the photometry process in the AIP4WIN (Astronomical Image Processing For Windows) software, it will give you C2-C1 data and V-C1 data. Studying and graphing this data as a function of time helps us know if there is any variability in the variable star that we chose.

V-C mag	K-C mag	Julian Day
4.068	5.345	2459503.884
4.08	5.439	2459503.884
3.988	5.358	2459503.884
3.947	5.262	2459503.884
3.976	5.253	2459503.884
4.124	5.419	2459503.884
4.117	5.408	2459503.885
4.074	5.39	2459503.885
4.05	5.37	2459503.885
4.009	5.435	2459503.885
3.936	5.274	2459503.885
3.98	5.297	2459503.885
4.101	5.493	2459503.886
4.142	5.499	2459503.886
4.054	5.361	2459503.886
4.124	5.437	2459503.886
4.065	5.445	2459503.886
4.07	5.43	2459503.886
4.004	5.333	2459503.887
4.123	5.46	2459503.887
4.114	5.423	2459503.887
4.106	5.467	2459503.887
4.117	5.509	2459503.887
4.133	5.505	2459503.887
4.128	5.528	2459503.888

Figure 9: Example of time-resolved photometry of S Fornacis.

2.3 RESIDUAL PLOTS

In the realm of data analysis, the residual plot stands out as a handy tool. It's essentially a visual chart that showcases the differences between what we observe and what our regression model predicts. On this chart, the vertical axis represents these

differences, or residuals, while the horizontal axis displays the independent variable. This setup is particularly useful for spotting issues like heteroscedasticity, non-linearity, and those pesky outliers in our data. If we see these, it might hint that our regression model isn't quite up to the mark.

Now, diving a bit deeper: heteroscedasticity is when our residuals don't scatter evenly. Non-linearity, on the other hand, suggests that the relationship between our variables isn't a straight line. And outliers? Well, they're those data points that don't quite fit in with the rest. On our plot, heteroscedasticity might look like a fan, non-linearity like a curve, and outliers as lone points far from the main cluster. The spread of our residuals can also tell us about data variability. A broader spread means more variability. Ideally, we want our residuals to scatter randomly around zero without forming any clear patterns. If that's the case, it's a good sign that our model is on the right track. Otherwise, it might be missing some key aspects of variability (Statistics How To. 2023).

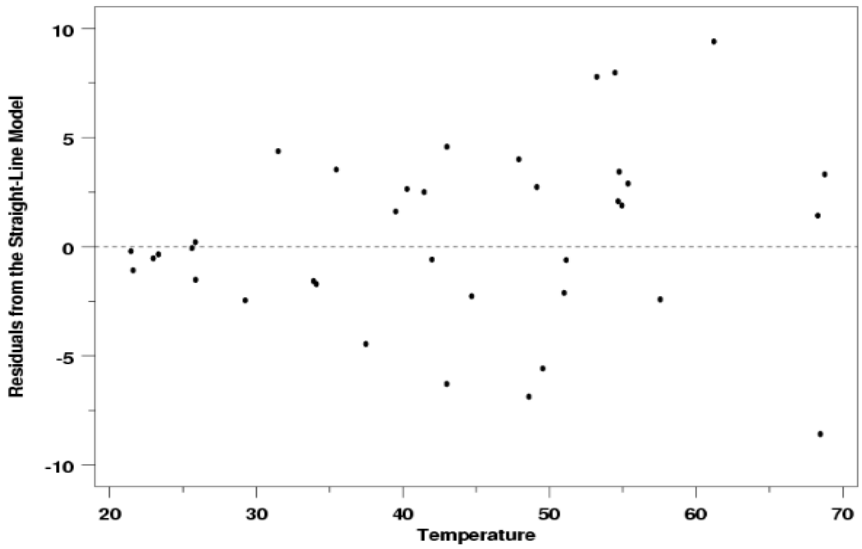

Figure 10: Residual plot showing cone-shaped spread (heteroscedasticity) showing variability in the data. (From: Statistics How To. (2023).

2.4 LIGHT CURVE

In astrophysics, light curves show how bright a star or planet is over time, helping to understand various space events. They reveal patterns from spinning stars, star flares, or even finding new planets when they pass in front of stars. Light curves are key in studying stars that change brightness, revealing natural pulses or things like eclipses. Explosive events, like big star explosions or gamma-ray bursts, show quickly changing light curves, giving clues about the explosion and the original star. They also help understand complex events like black holes pulling in stars, shown by the EGRET map that captures γ-ray emission.

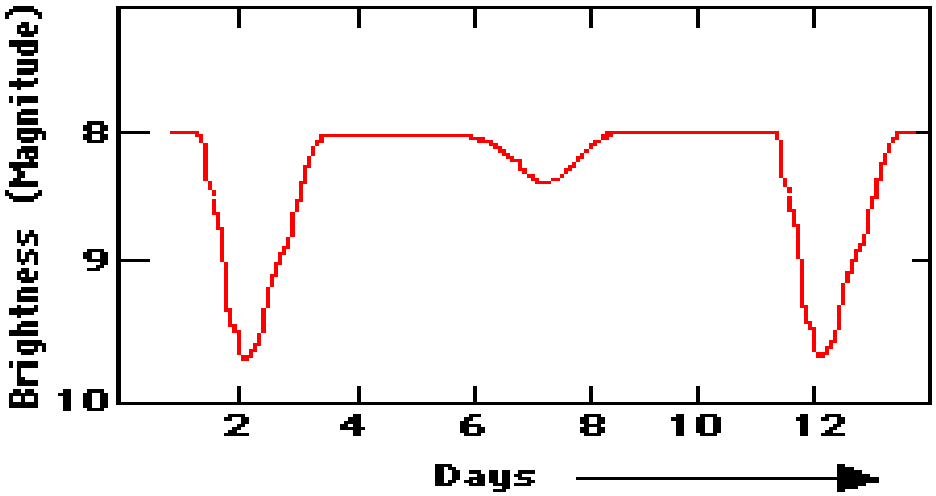

Figure 11: Sample light curve of an eclipsing binary star system (Newman 2020).

2.5 CALCIUM K FILTER

In the field of astrophysics, a filter known as Calcium K (Ca K) is employed to target a layer of the Sun that resides below and is slightly cooler than the layer observed at the hydrogen-alpha wavelength of 656.3 nm. The Ca K emission line emerges at the violet end of the Sun's visible spectrum, specifically at the relatively short wavelength of

393.4 nm. This spectral line is a strong indicator of magnetic activity in the chromosphere and is linked with the chromospheric network.

While the primary function of a Ca K filter is generally accepted to be for imaging purposes, there are a few observers who have successfully utilized it for visual observation at this wavelength. The resulting image appears as an ethereal purple disk, teetering on the edge of human visual perception. Our eyes' sensitivity to this wavelength can vary greatly and tends to diminish with age, meaning the image may not be discernible to all observers. Intriguingly, some individuals have noted an unexpected enhancement in their ability to perceive the Ca K view following laser eye surgery, which was originally performed for medical reasons (Rix et al. 2015).

3.ANALYSIS

3.1 S FORNACIS

On a particular evening, March 6, 1899, the sky presented an interesting spectacle. A newly spotted comet was making its journey through the Fornax constellation, heading towards a region where the star S Fornacis resides. That night, four seasoned observers decided to take a closer look at this celestial event.
Interestingly, as the evening progressed, three of these observers—one from Austria, another from Italy, and the third from Germany—noticed something unusual. To their surprise, S Fornacis appeared much brighter than usual. They estimated, just by looking, that it was shining almost 15 times its usual brightness. What's even more intriguing is that all three of them observed this unusual brightness within a short span of 17 minutes. However, not all shared this observation. Another observer from Italy, who had looked at the star and the comet just about 30 minutes before the others, didn't notice anything out of the ordinary with S Fornacis. Additionally, a photograph taken at Harvard Observatory

later that night showed S Fornacis in its usual state. Now, while these observations from over a century ago rely on human eyes and might have their limitations, the fact that three observers from different locations noticed the same thing gives some weight to their claims.

In this paper, we try to analyze and study photometry data and light curves from S Fornacis taken with the Sierra Remote Observatory and try to have a go at solving the mystery of whether or not S Fornacis is variable or not.

3.2 TIME-RESOLVED PHOTOMETRY

Using the data from Sierra Remote observatory taken by Dr. Frederick Ringwald, I have used AIP4WIN software to get photometry data of the star S For. Given below are the Check Star-Comparison star (K-C) and Variable Star - Comparison star (V-C) data as a function of time for different days. The days below are in Julian days format. Firstly, we will try to analyze the light curves extracted from this data.

3.3 LIGHT CURVES OF S FORNACIS

1) Date: 2021 October 15-16

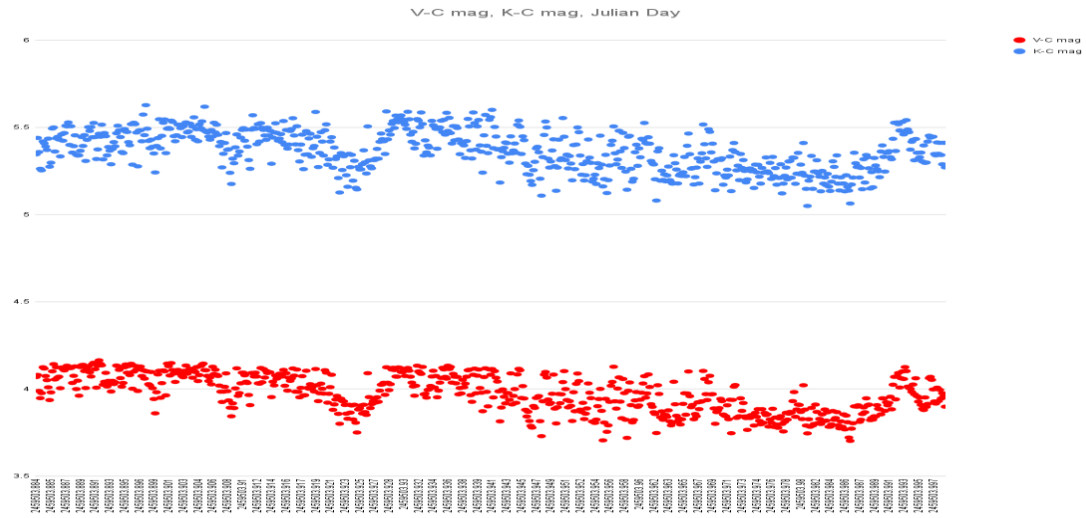

Figure 12: Time-resolved photometry of S Fornacis on 2021 October 15-16

2) Date: 2021 October 16-17

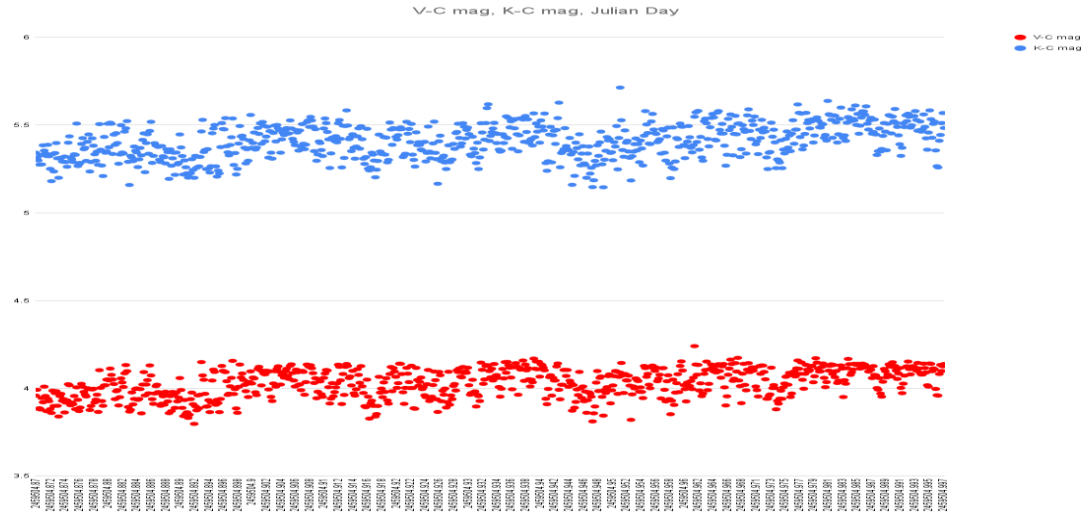

Figure 13: Time-resolved photometry of S Fornacis on 2021 October 16-17

3) Date: 2021 October 29-30

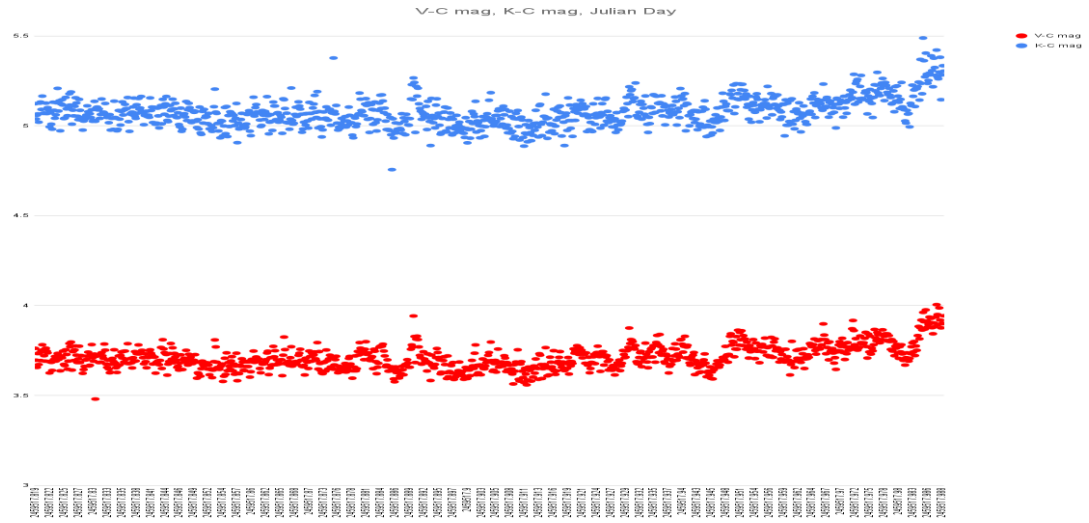

Figure 14: Time-resolved photometry of S Fornacis on 2021 October 29-30

4) Date: 2021 November 11-12

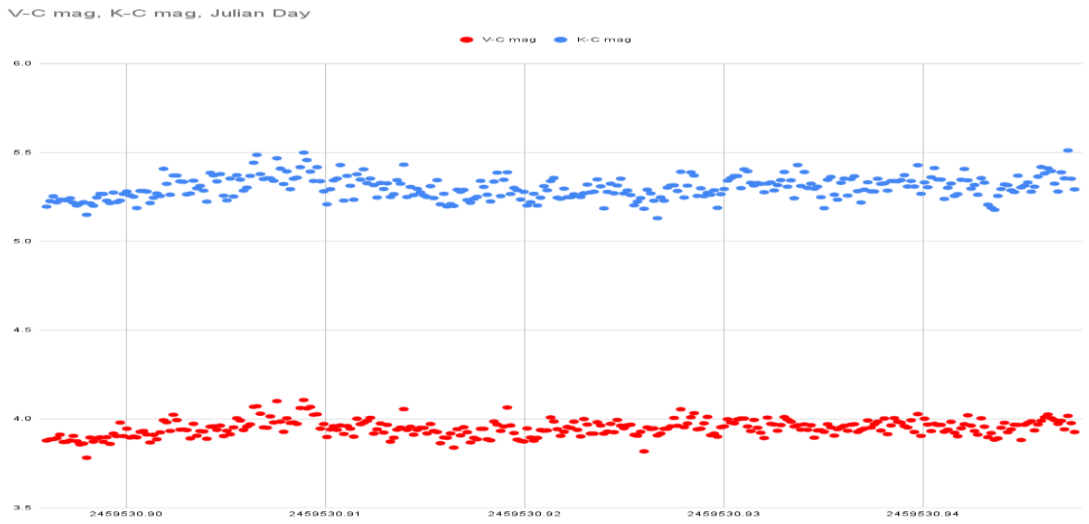

Figure 15: Time-resolved photometry of S Fornacis on 2021 November 11-12

5) Date: 2021 November 12-13

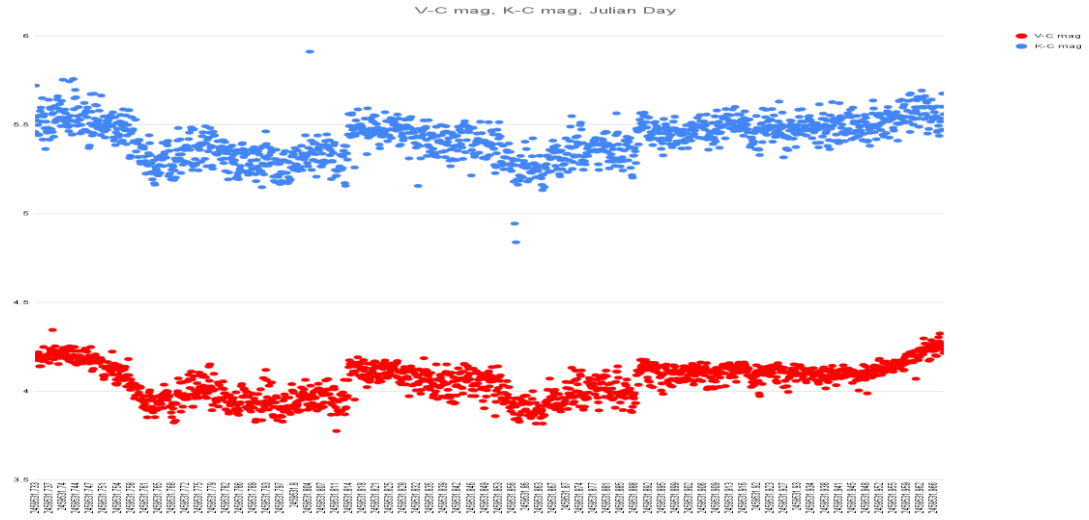

Figure 16: Time-resolved photometry of S Fornacis on 2021 November 12-13

6) Date: 2021 November 13-14

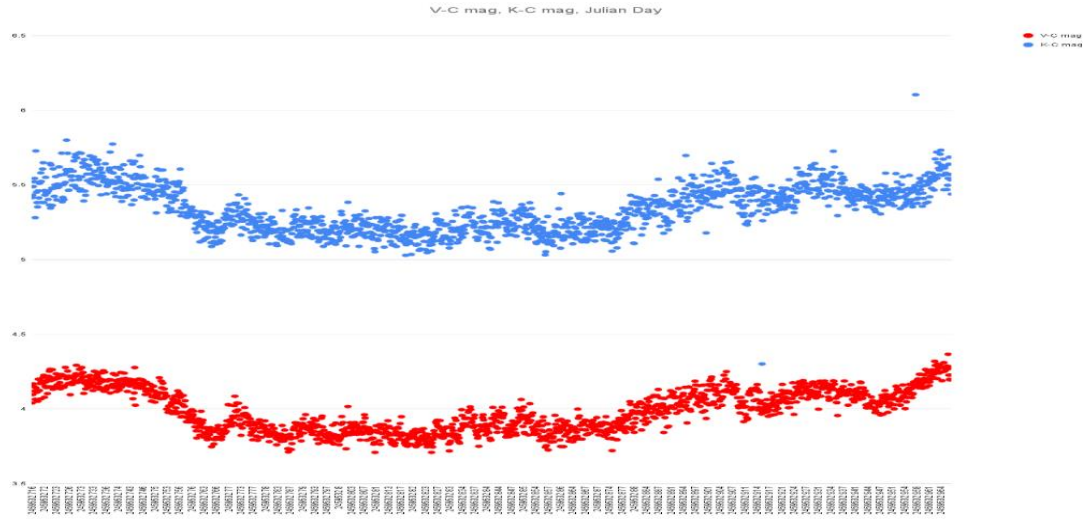

Figure 17: Time-resolved photometry of S Fornacis on 2021 November 13-14

7) Date: 2021 November 21-22

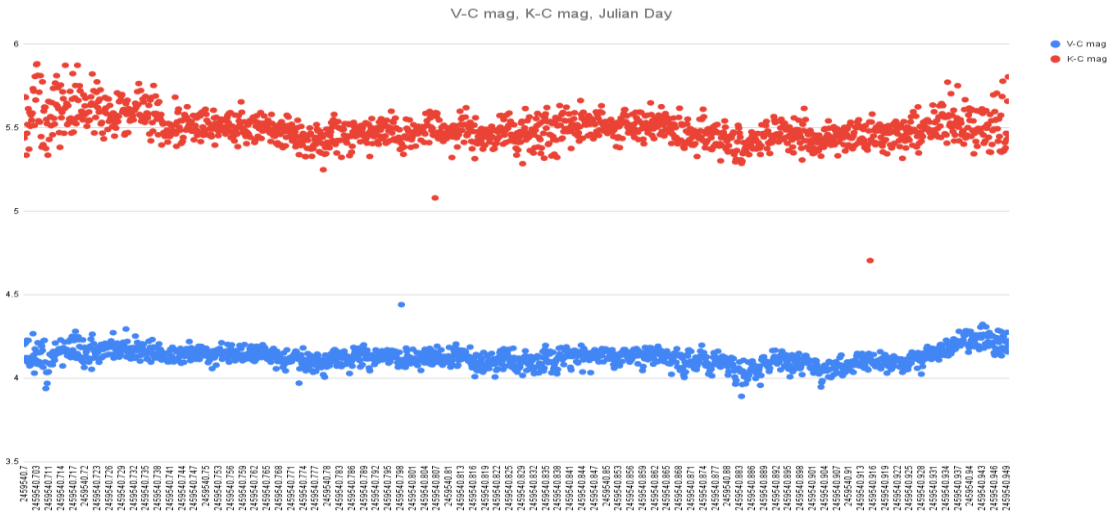

Figure 18: Time-resolved photometry analysis of S Fornacis on 2021 November 21-22

The light curves plotted above are apparent magnitudes for (Variable Star – Comparison Star), which are plotted as blue dots throughout this thesis. Apparent magnitudes for (Check Star – Comparison Star) plotted as red dots. If there is variability in the comparison star we are analyzing, the pattern of red dots will be almost like a straight line and the pattern of blue dots will have an increasing or decreasing curve.

As observed through visual analysis, none of the S Fornacis curves show any apparent variability.

3.4 RESIDUAL PLOTS OF S FORNACIS

1) Date: 2021 October 15-16

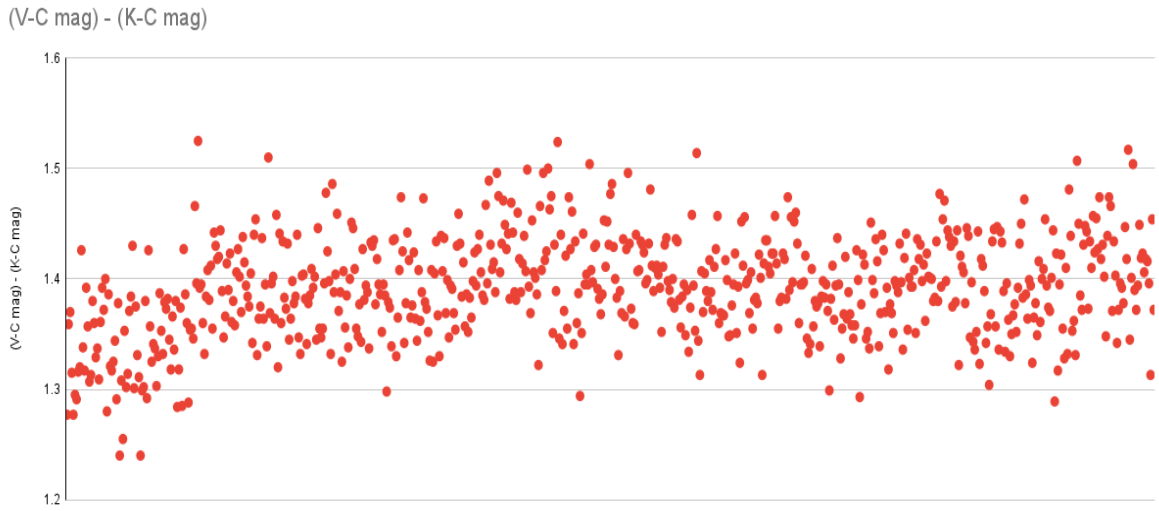

Figure 19: Residual plot of S Fornacis taken on 2021 October 15-16.

2) Date: 2021 October 16-17

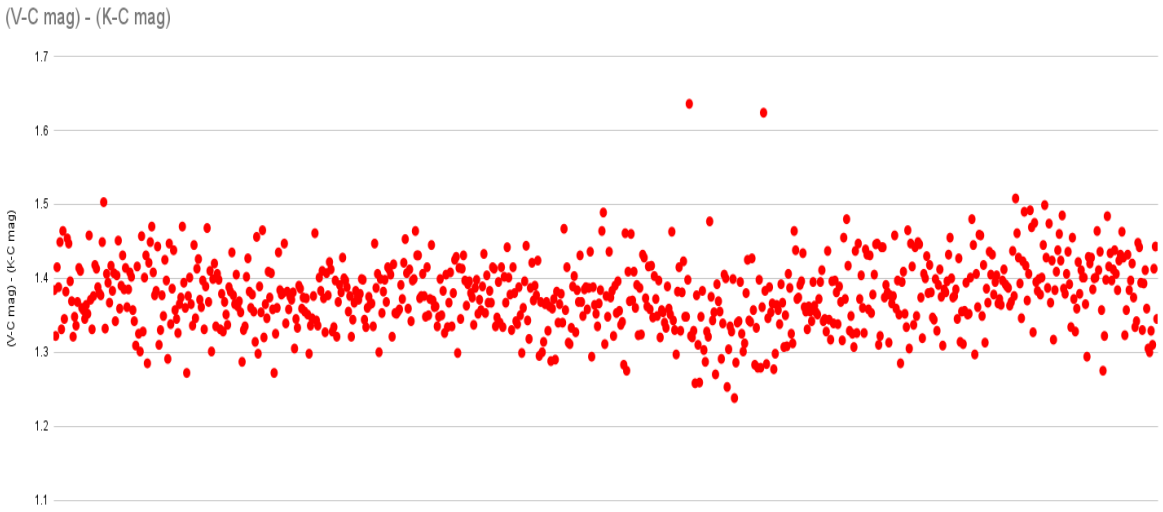

Figure 20: Residual plot of S Fornacis taken on 2021 October 16-17.

3) Date: 2021 October 29-30

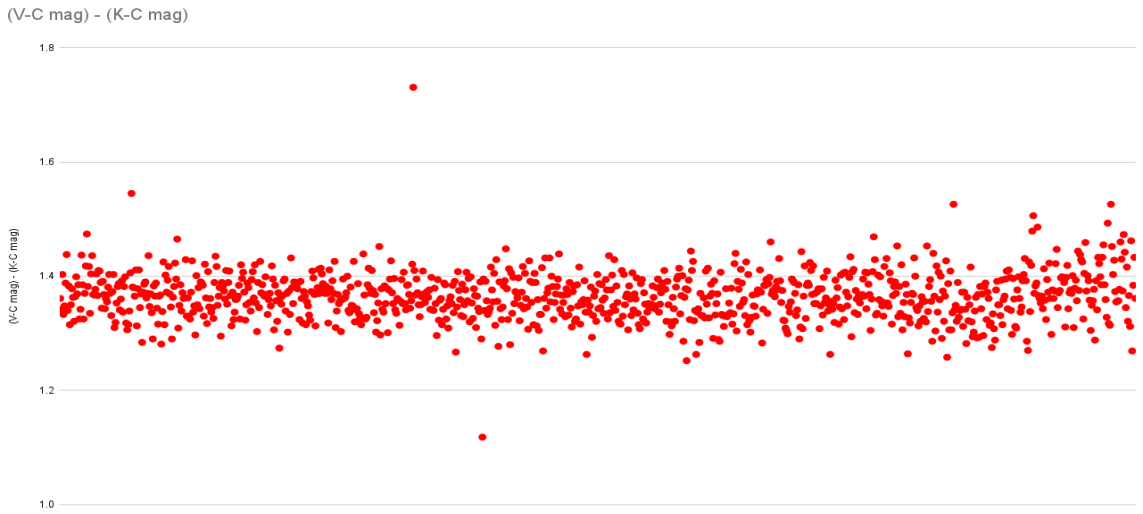

Figure 21: Residual plot of S Fornacis taken on 2021 October 29-30.

4) Date: 2021 November 11-12

Figure 22: Residual plot of S Fornacis taken on 2021 November 11-12.

5) Date: 2021 November 13-14

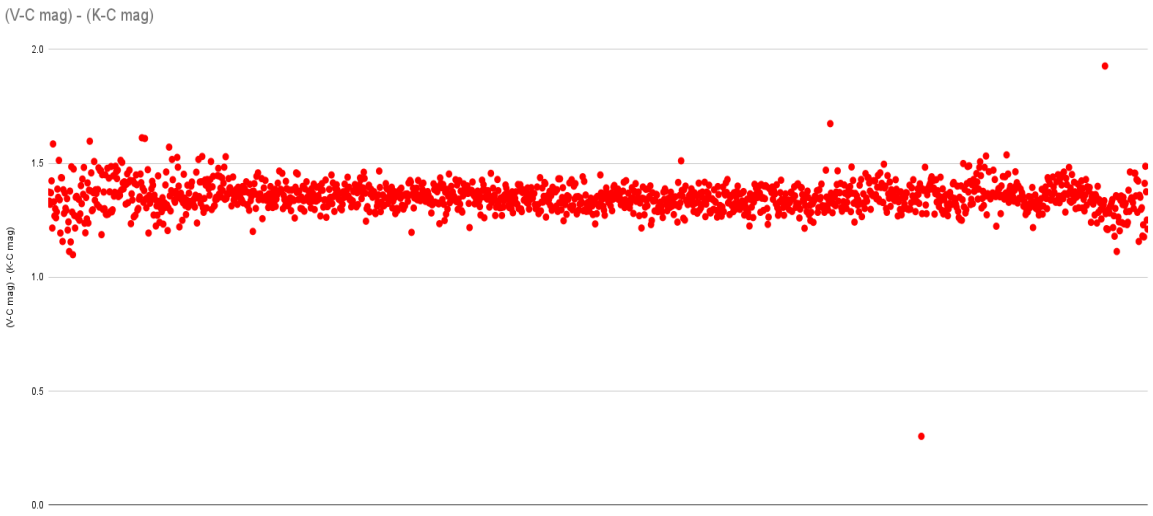

Figure 23: Residual plot of S Fornacis taken on 2021 November 13-14.

6) Date: 2021 November 21-22

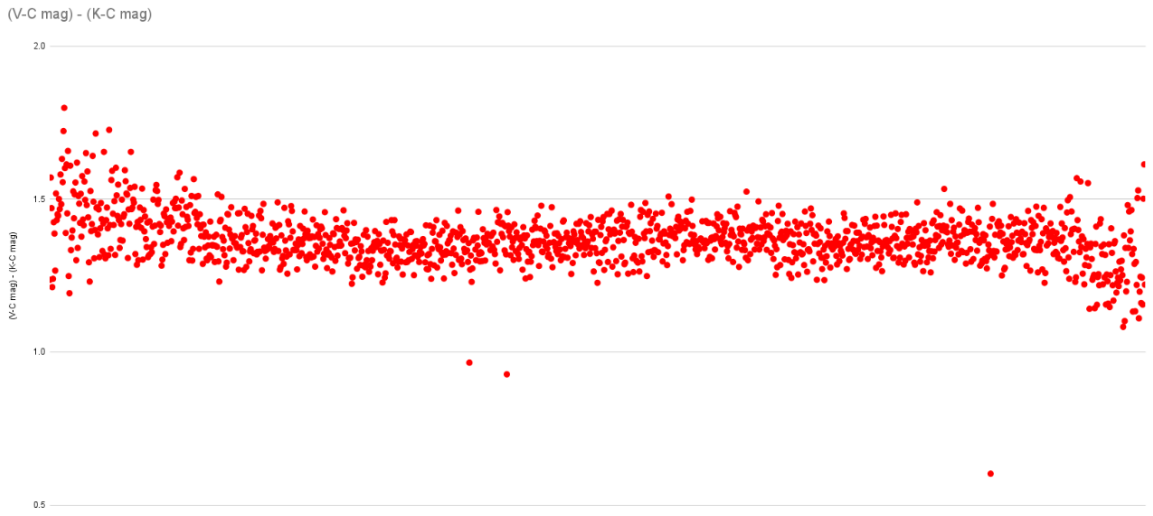

Figure 24: Residual plot of S Fornacis taken on 2021 November 21-22.

A visual inspection of residual plots of S Fornacis shows up that there is no apparent variability in the magnitude observed.

3.5 HD 209458

HD 209458, a G0V star similar to our Sun, is an 8th-magnitude celestial object located in the Pegasus constellation. Being approximately 159 light-years away, it's not visible to the naked eye but can be easily spotted with good binoculars or a small telescope.

In 1999, two separate research groups independently discovered an exoplanet in orbit around this star using the radial velocity method. Shortly after this discovery, additional teams observed a transit of the planet across the star's surface, marking it as the first identified transiting exoplanet, now known as HD 209458 b (see Brown et al. 2001 and references therein).

As HD 209458 b orbits and transits its host star, it causes a roughly 2% dimming of the star's light every 3.5 days, classifying HD 209458 as an extrinsic variable star. Under the variable star designation, it's referred to as V376 Pegasi. It also serves as the prototype for the "EP" category in the General Catalog of Variable Stars, a classification attributed to stars that exhibit eclipses due to their orbiting planets (Lines et al. 2018).

3.6 TIME-RESOLVED PHOTOMETRY OF HD 209458

1) Date: 2021 September 28-29

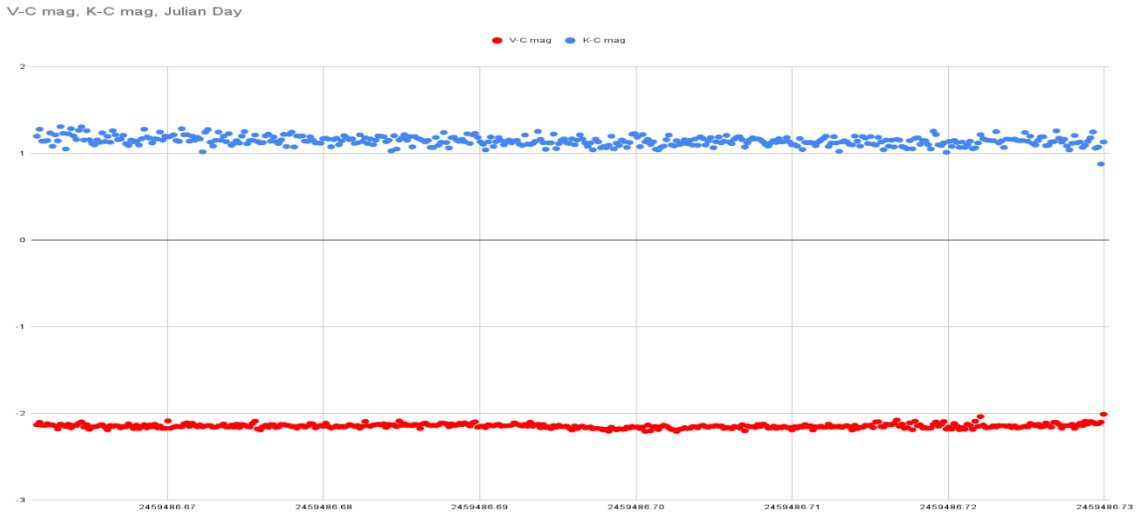

Figure 25: Time-resolved photometry of HD 209458 on 2021 September 28-29

2) Date: 2021 September 29-30

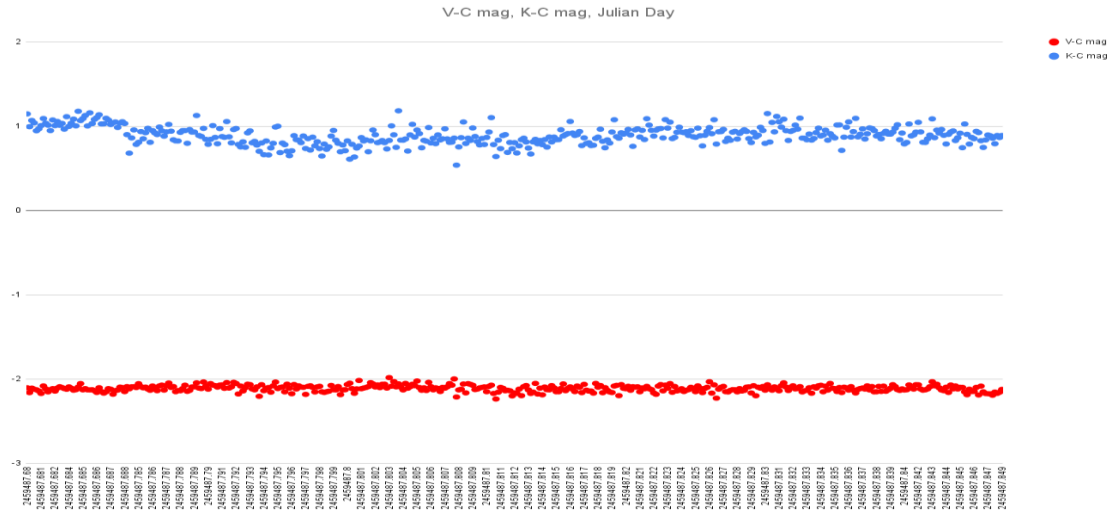

Figure 26: Time-resolved photometry of HD 209458 on 2021 September 29-30

3) Date: 2021 October 07-08

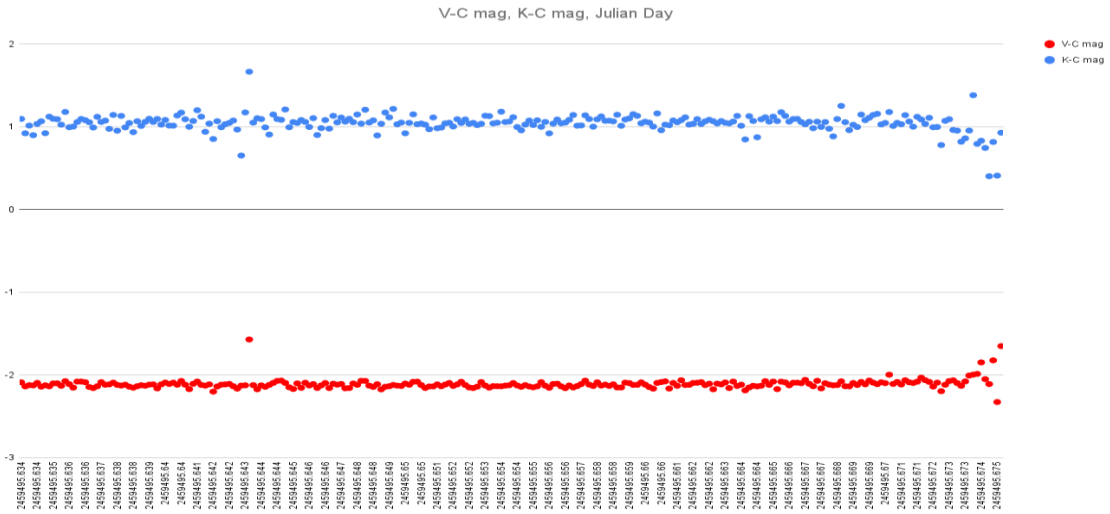

Figure 27: Time-resolved photometry of HD 209458 on 2021 October 07-08

4) Date: 2021 October 09-10

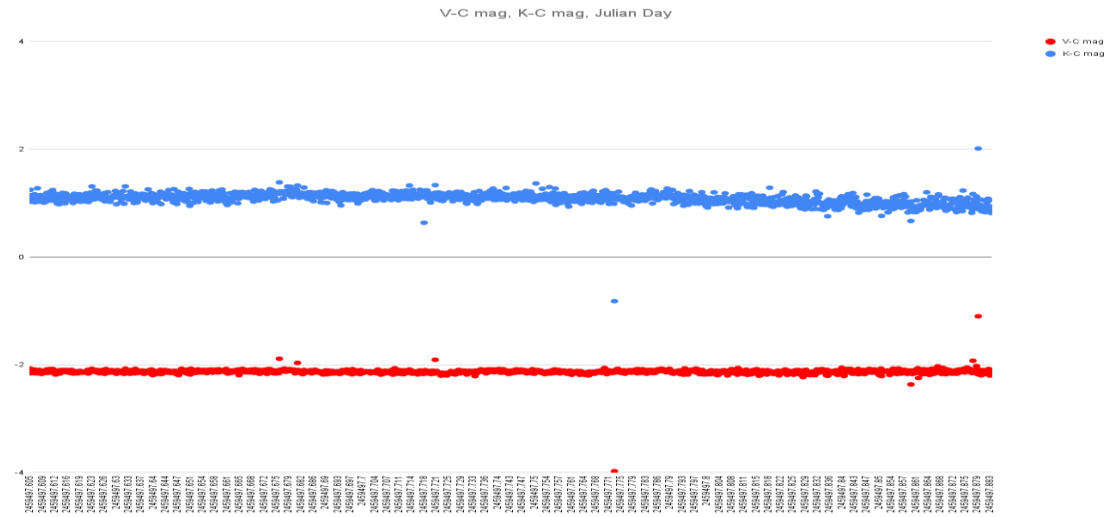

Figure 28: Time-resolved photometry of HD 209458 on 2021 October 09-10

5) Date: 2021 October 10-11

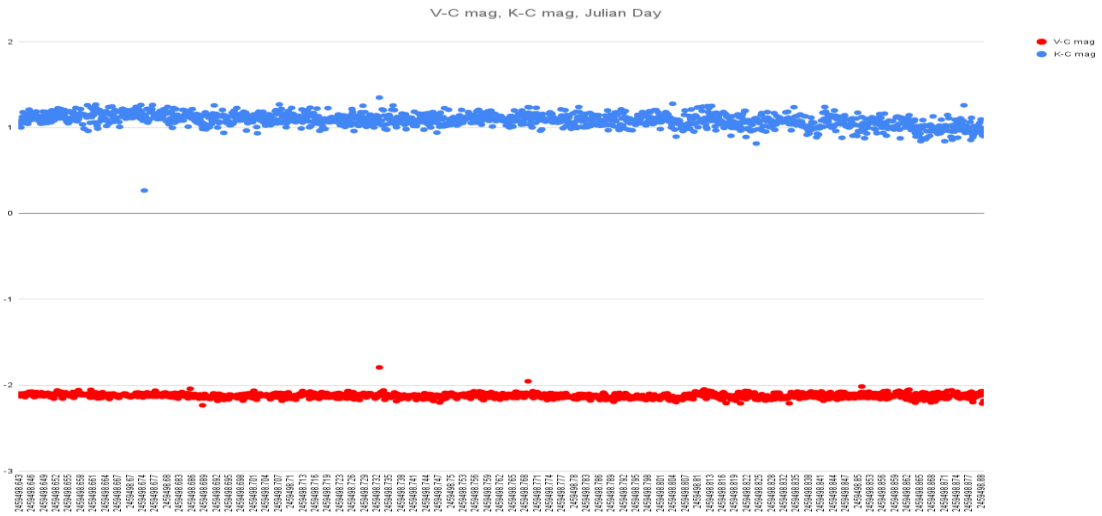

Figure 29: Time-resolved photometry of HD 209458 on 2021 October 10-11

6) Date: 2021 October 13-14

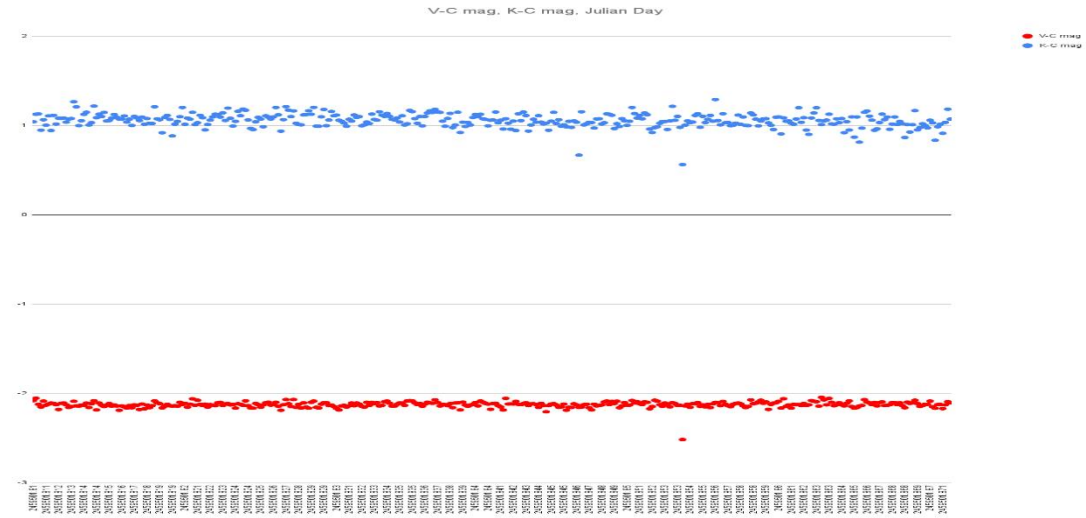

Figure 30: Time-resolved photometry of HD 209458 on 2021 October 13-14

7) Date: 2021 October 14-15

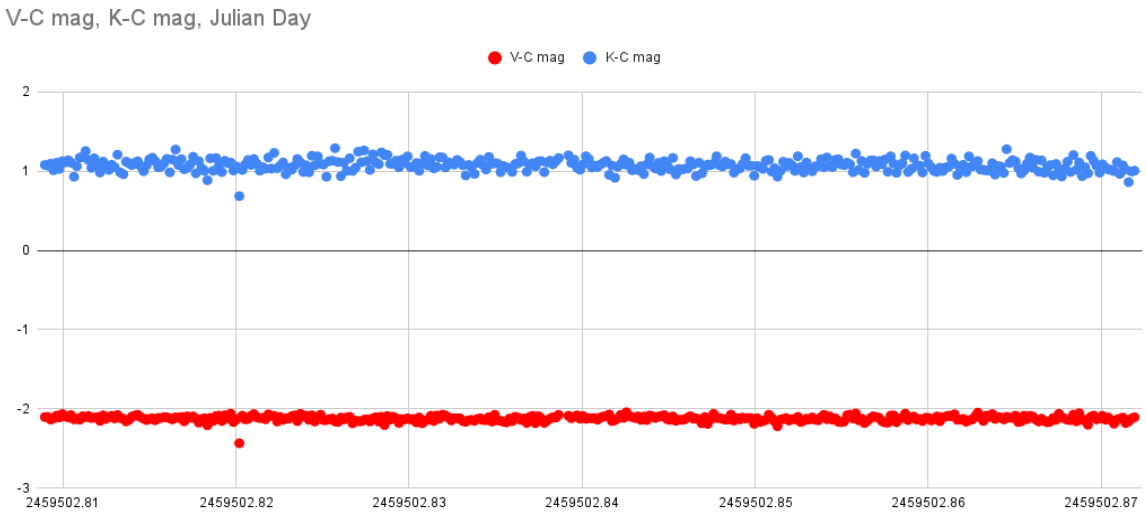

Figure 31: Time-resolved photometry of HD 209458 on 2021 October 14-15

HD209458 is a star which has been observed to be variable (Brown et al. 2001), but unfortunately through our visual analysis of the light curves of HD209458, we are unable to discern any apparent variability.

3.7 RESIDUAL PLOTS OF HD209458

1) Date: 2021 September 28-29.

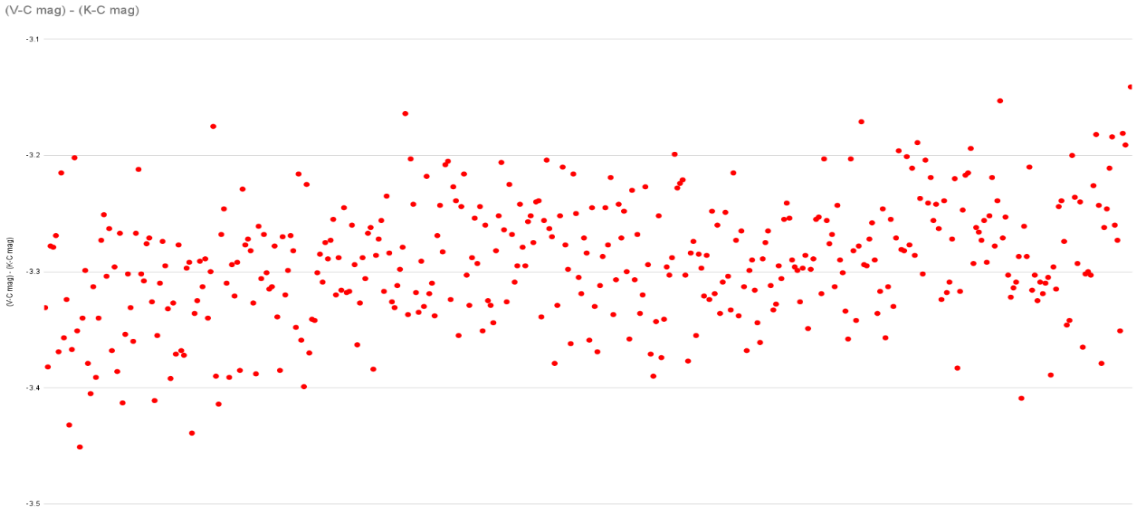

Figure 32: Residual plot of HD209458 taken on 2021 September 28-29.

2) Date: 2021 September 29-30

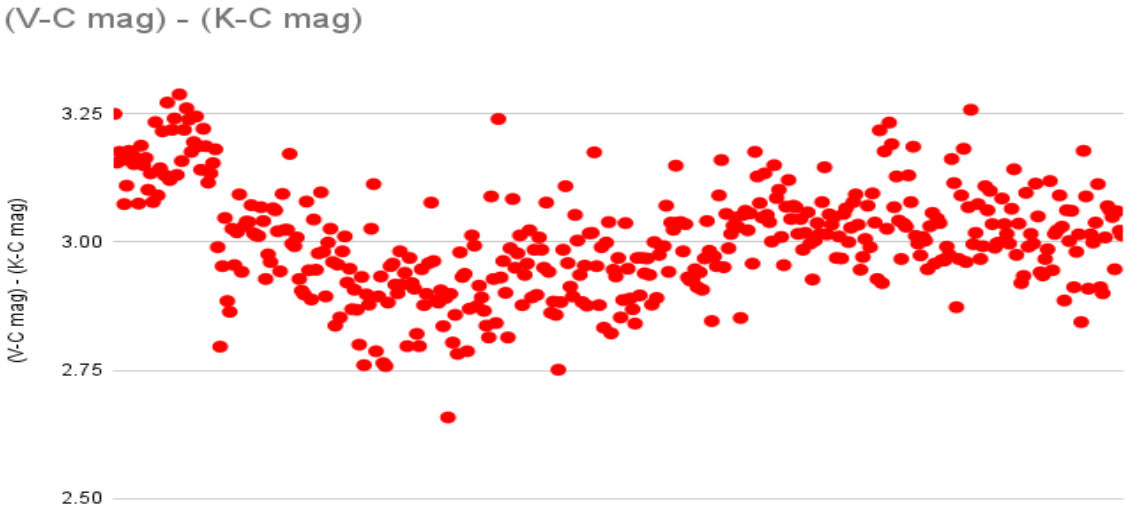

Figure 33: Residual plot of HD209458 taken on 2021 September 29-30.

3) Date: 2021 October 07-08

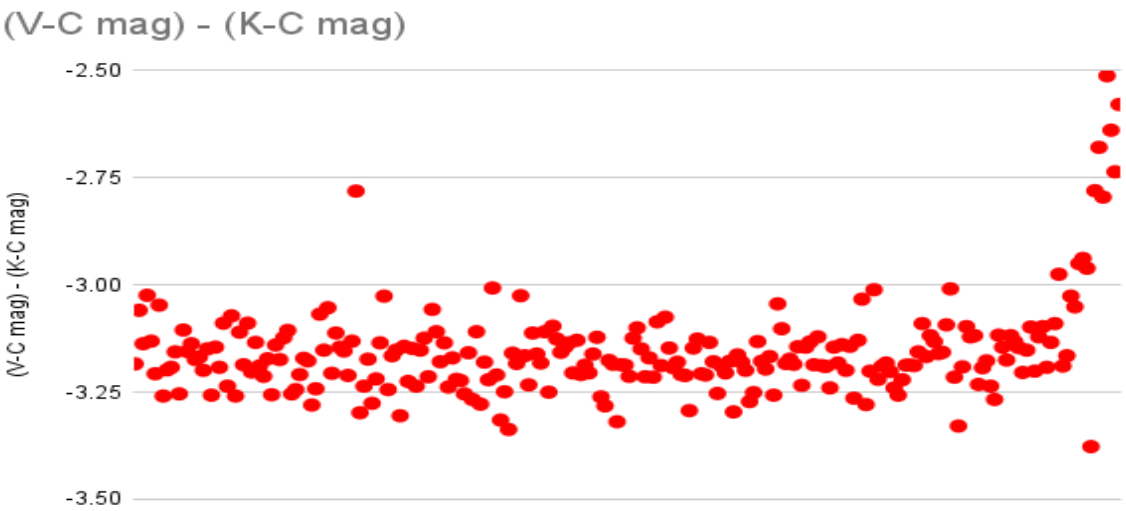

Figure 34: Residual plot of HD209458 taken on 2021 October 07-08.

4) Date: 2021 October 09-10

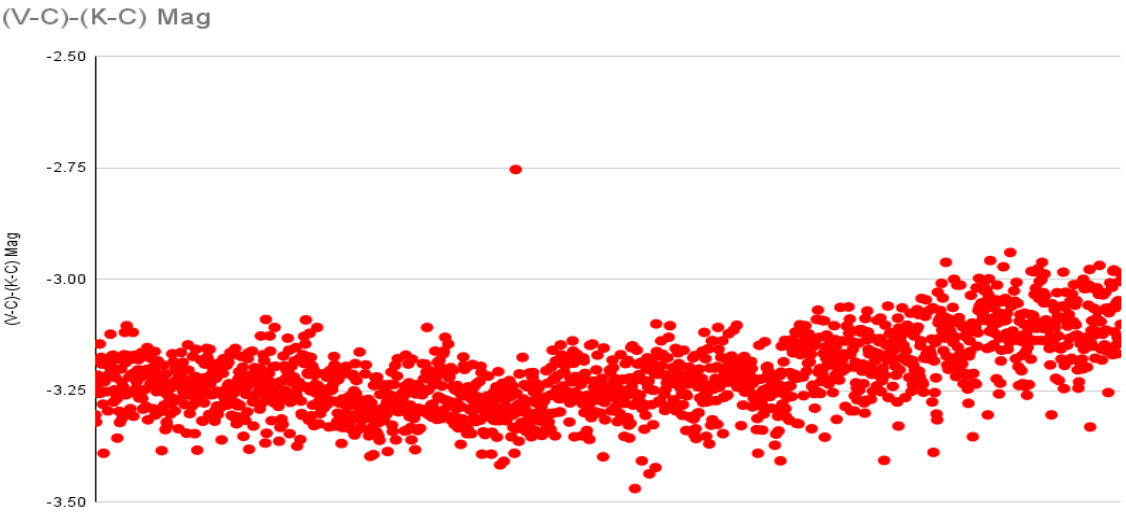

Figure 35: Residual plot of HD209458 taken on 2021 October 09-10.

5) Date: 2021 October 10-11

Figure 36: Residual plot of HD209458 taken on 2021 October 10-11.

6) Date: 2021 October 13-14

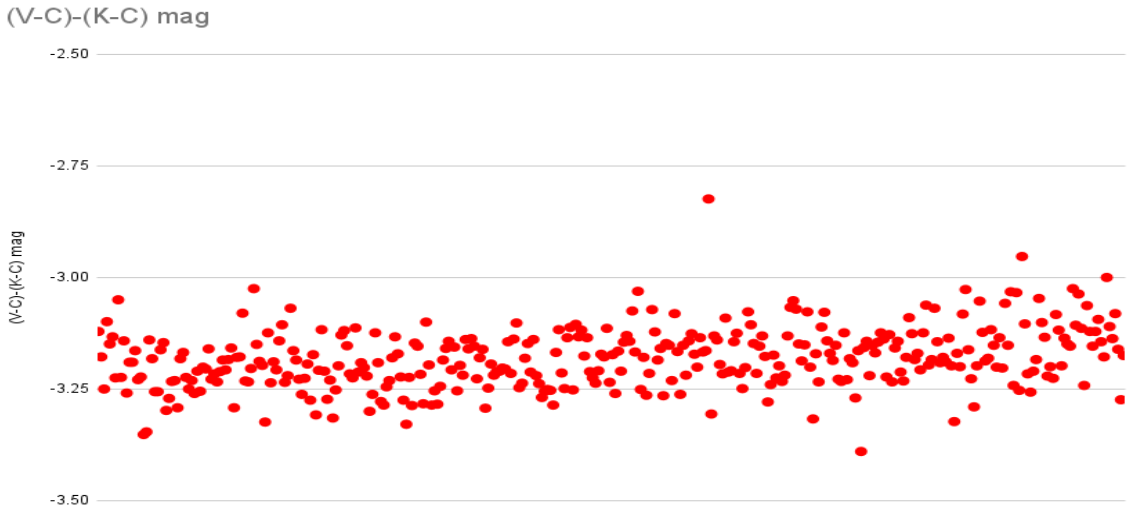

Figure 37: Residual plot of HD209458 taken on 2021 October 13-14.

7) Date: 2021 October 14-15

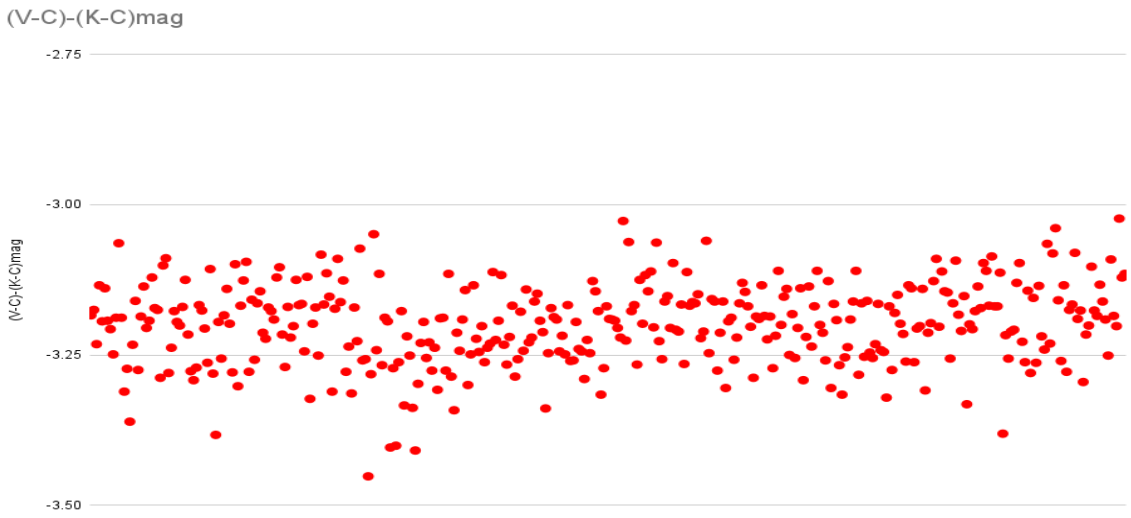

Figure 38: Residual plot of HD209458 taken on 2021 October 14-15.

Residual plots with variability have a pattern associated with them, through visual analysis it is certain the residual plots of HD209458 show no variability.

3.8 CONCLUSION ABOUT TIME-RESOLVED PHOTOMETRY

The time-resolved photometry conducted on the stars S Fornacis and HD209458 offers valuable insights into their nature and variability. After a comprehensive examination of the light curves for both V-C mag and K-C mag, it has become apparent that there is minimal variability in their luminosity. Particularly, the V-C mag demonstrates an almost linear pattern, indicating a steady light output. This lack of significant variability can have various implications, including the stability of these stars and their stage in stellar evolution.

3.9 LOMB-SCARGLE PERIODOGRAM

The Lomb-Scargle periodogram is a renowned algorithm used for identifying and analyzing periodic signals within time-series data that is irregularly sampled. This method calculates an estimate of the power spectrum akin to Fourier, derived from such data, and it also has the ability to evaluate the significance of faint periodic signals. The Lomb-Scargle periodogram can be either normalized or unnormalized, contingent upon the reference model, and various versions of this periodogram exist, including an efficient implementation by Press & Rybicki (1989). This technique finds extensive use in the field of astronomy, with applications spanning the analysis of radial velocity data to the investigation of pulsating variable stars (VanderPlas 2018).

3.10 LOMB-SCARGLE PERIODOGRAM USING PYTHON

I've developed a Python-based program using the Lomb-Scargle periodogram to detect and analyze stellar brightness variability, a key aspect in studying phenomena such as variable stars and exoplanetary transits.

1) HD 209458:

a) Time-resolved photometry periodogram

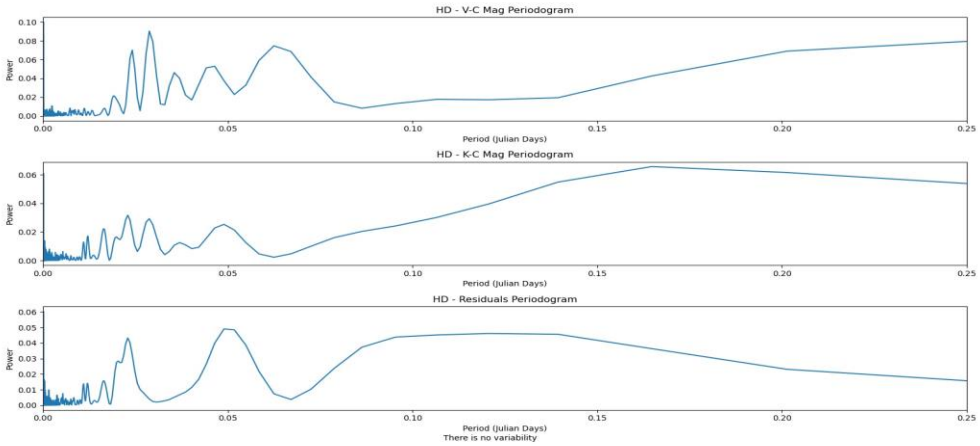

Figure 39: Time-resolved photometry periodogram for HD 209458: Approximate Power vs Period

b) Time-resolved photometry frequency periodogram

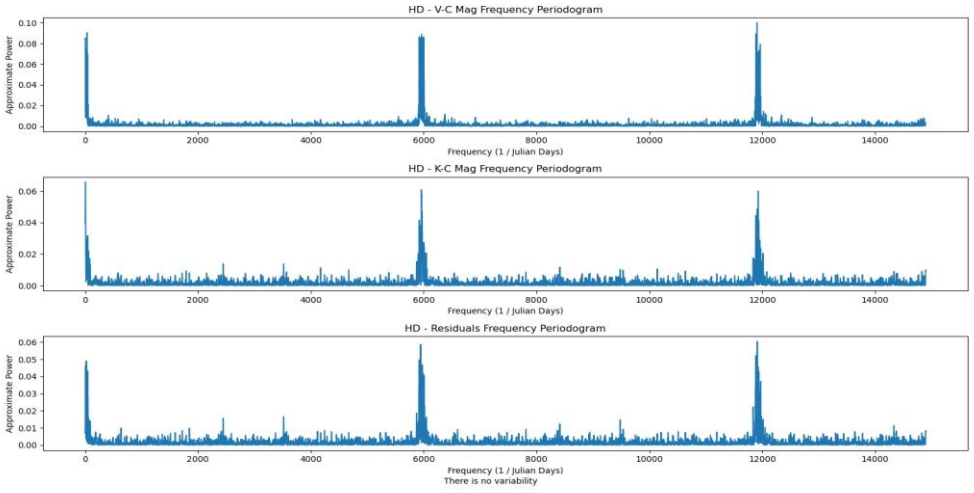

Figure 40: Tim-resolved photometry frequency periodogram for HD 209458: Approximate Power vs Period

2) S Fornacis:

a) Time-resolved photometry periodogram

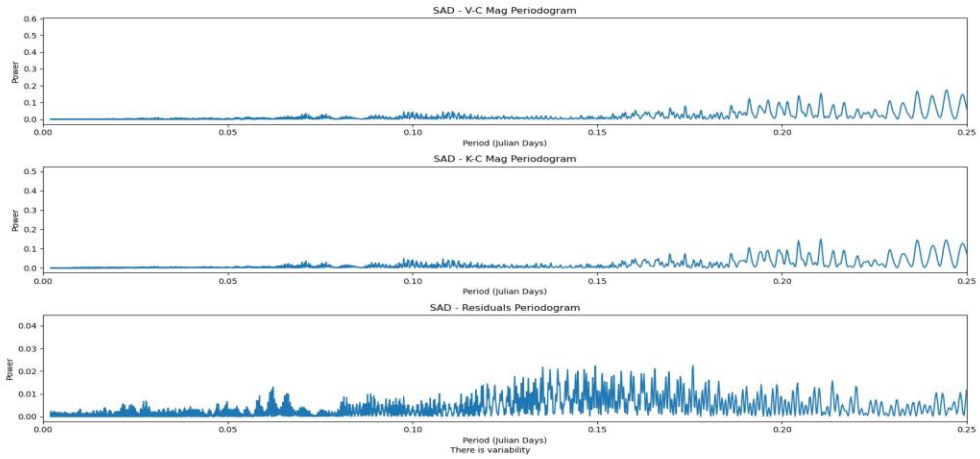

Figure 41: Time-resolved photometry periodogram for S Fornacis: Approximate Power vs Period

b) Time-resolved photometry frequency periodogram

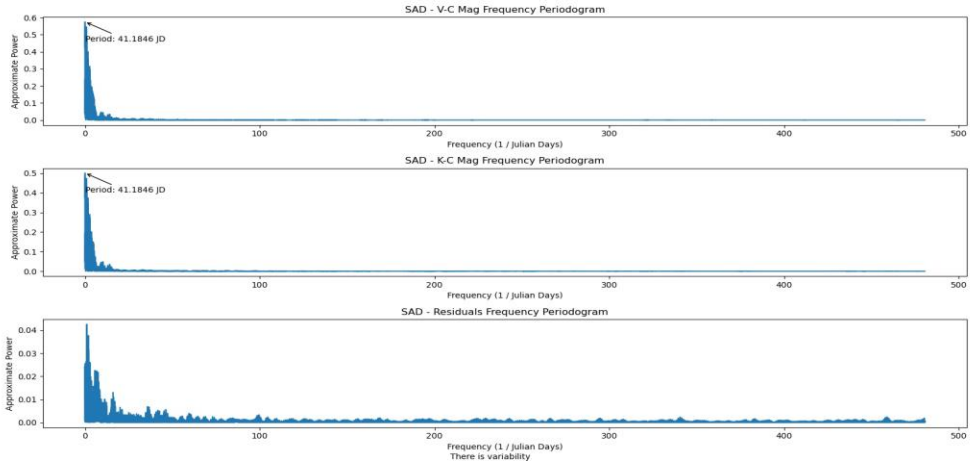

Figure 42: Time-resolved photometry frequency periodogram for S Fornacis: Approximate Power vs Period

The application of the Lomb-Scargle periodogram on the time-resolved photometry data has yielded intriguing results for S Fornacis and HD209458. While the data for HD209458 did not reveal any apparent periodicity, suggesting a lack of regular cyclic variations in its brightness, the situation was different for S Fornacis. The periodogram for S Fornacis demonstrated clear periodicity, indicating a consistent pattern of variability in its light output.

3.11 PERANSO

PERANSO is a light curve and period analysis software application used in astronomy. It offers a set of powerful analysis functions to work with large, multi-night astronomical data sets, collected by a variety of observers. It is equally effective for the individual observer, who wants to analyze his observations of one or more nights.

In all of the graphs below, the black dots represent the V-C magnitude and the red dots represent K-C magnitude.

3.12 ANALYSIS OF HD209458 USING PERANSO

Similar to the light curve analysis in the previous section, we subjected the time-resolved differential photometry data taken from Sierra Remote Observatory to light curve analysis through the PERANSO software. The results we get have to be visually analyzed, if there is magnetic variability the V-C magnitude will not be a straight line.

a) Light Curves for HD 209458:

1)

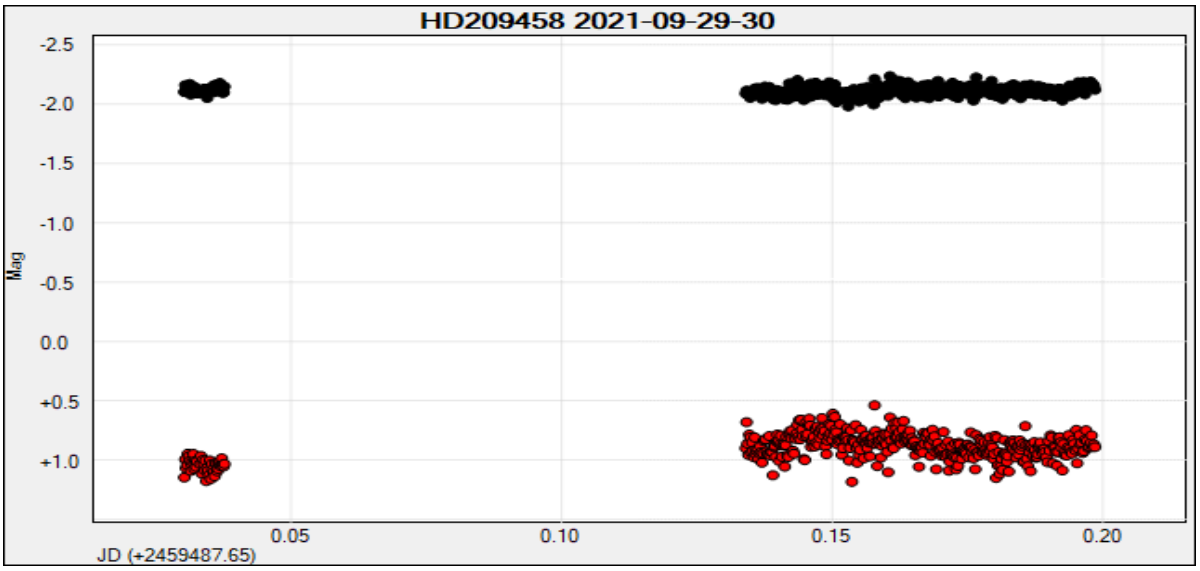

Figure 43: Light curves using PERANSO software for HD 209458 on 2021 September 29-30

2)

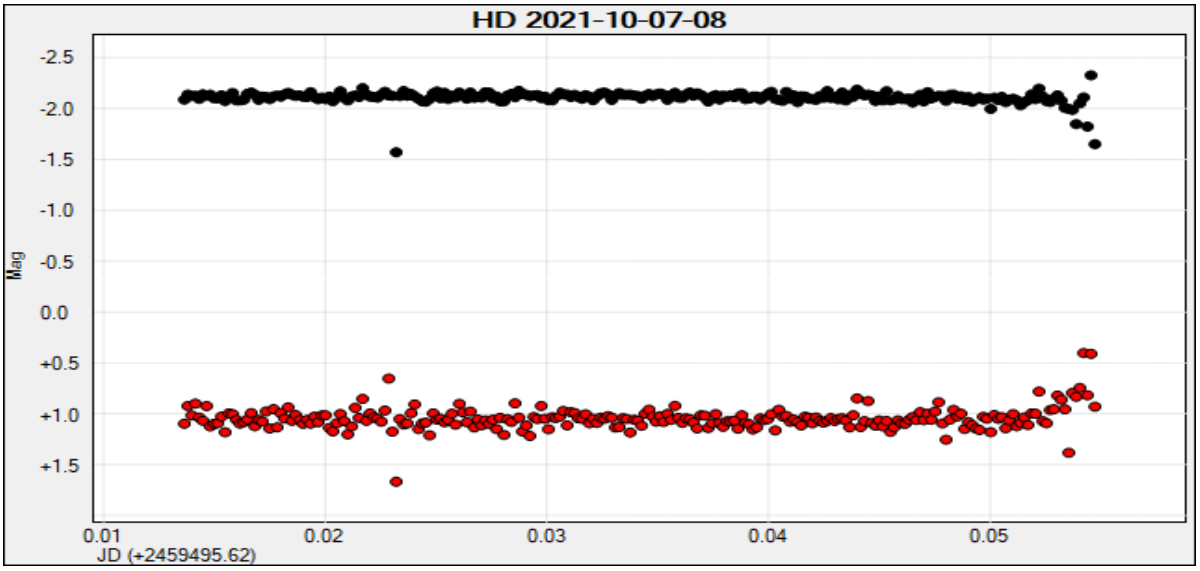

Figure 44: Light curves using PERANSO software for HD 209458 on 2021 October 07-08

3)

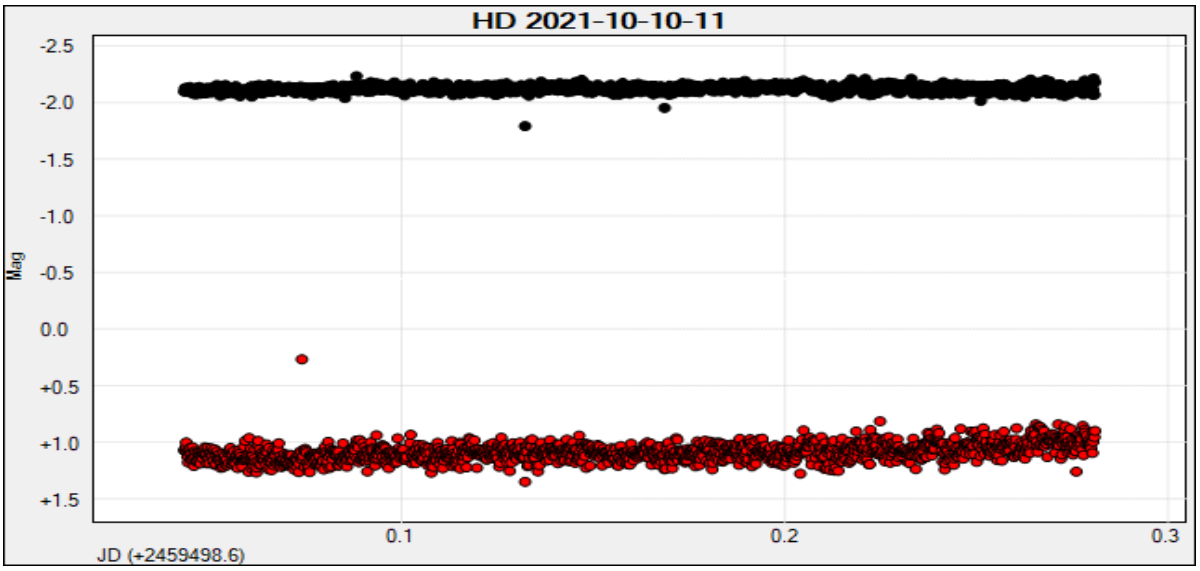

Figure 45: Light curves using PERANSO software for HD 209458 on 2021 October 10-11

4)

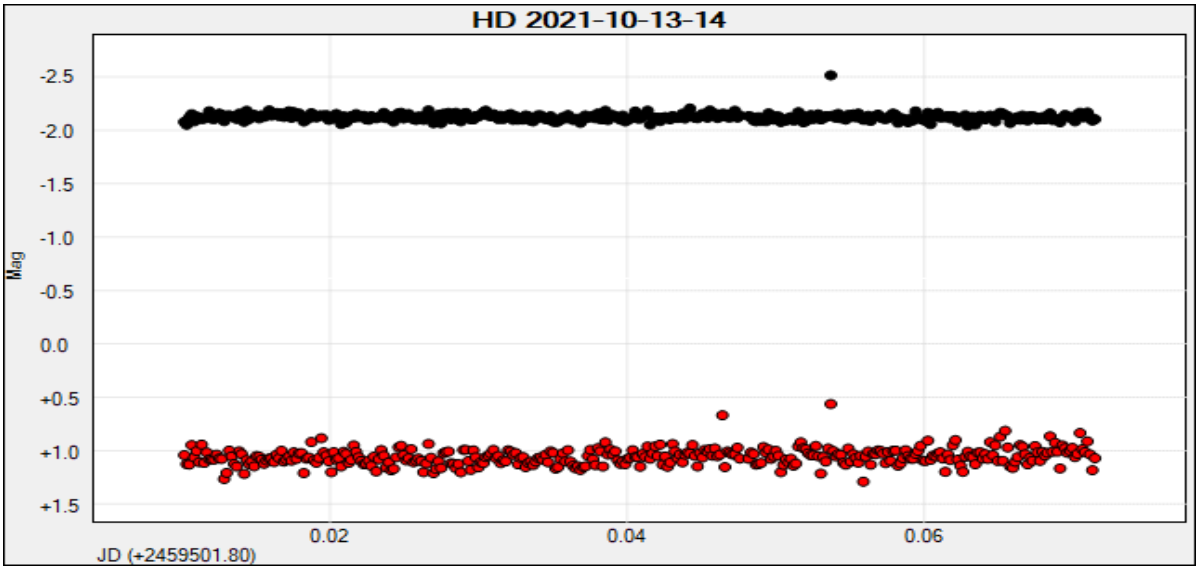

Figure 46: Light curves using PERANSO software for HD 209458 on 2021 October 13-14

5)

Figure 47: Light curves using PERANSO software for HD 209458 on 2021 October 19-20

After subjecting the time-resolved differential photometry data to light curve analysis in the PERANSO software, it is apparent that no variability is detected through this method in HD209458.

3.13 LOMB-SCARGLE PERIODOGRAM ANALYSIS FOR HD209458 BETWEEN 0.01-2 CYCLES PER DAY

The periodicity of HD209458 is 3.52 days (Brown et al. (2001). Twice this corresponds to a frequency of 0.1429 cycles/day. We are choosing the frequency between 0.01 to 2 cycles per day particularly to search for this periodicity.

1)

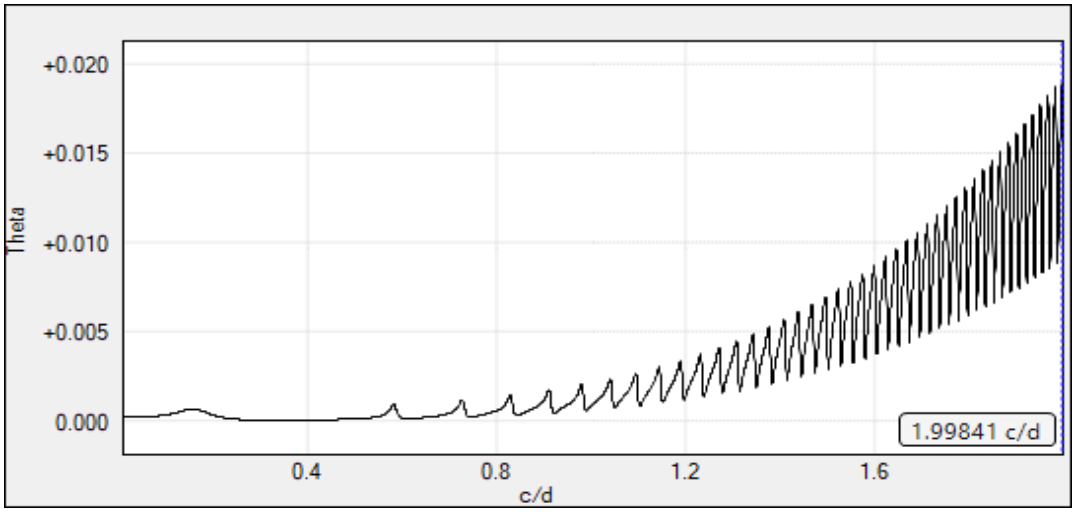

Figure 48: Lomb-Scargle periodogram using PERANSO software for HD 209458 on 2021 September 28-29

2)

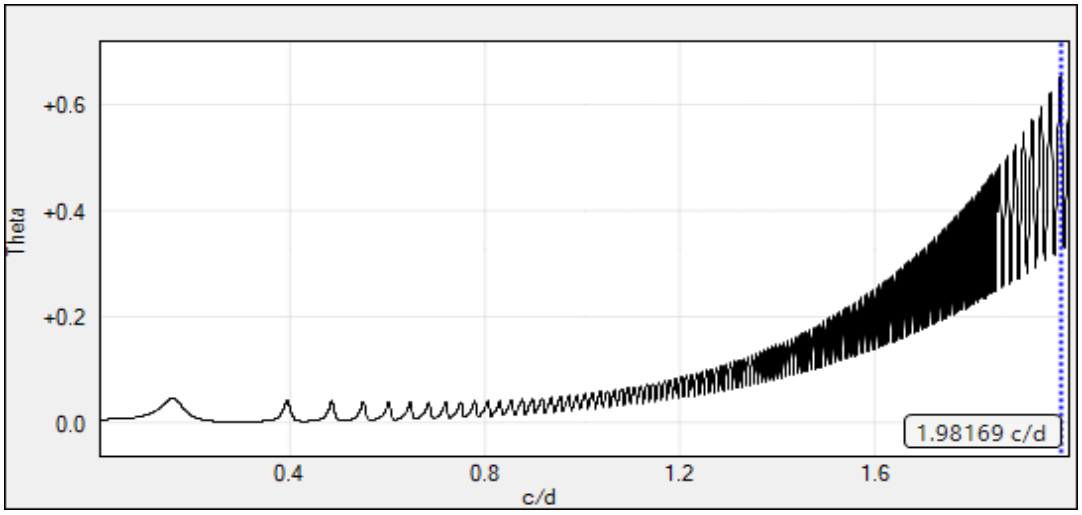

Figure 49: Lomb-Scargle periodogram using PERANSO software for HD 209458 on 2021 September 29-30

3)

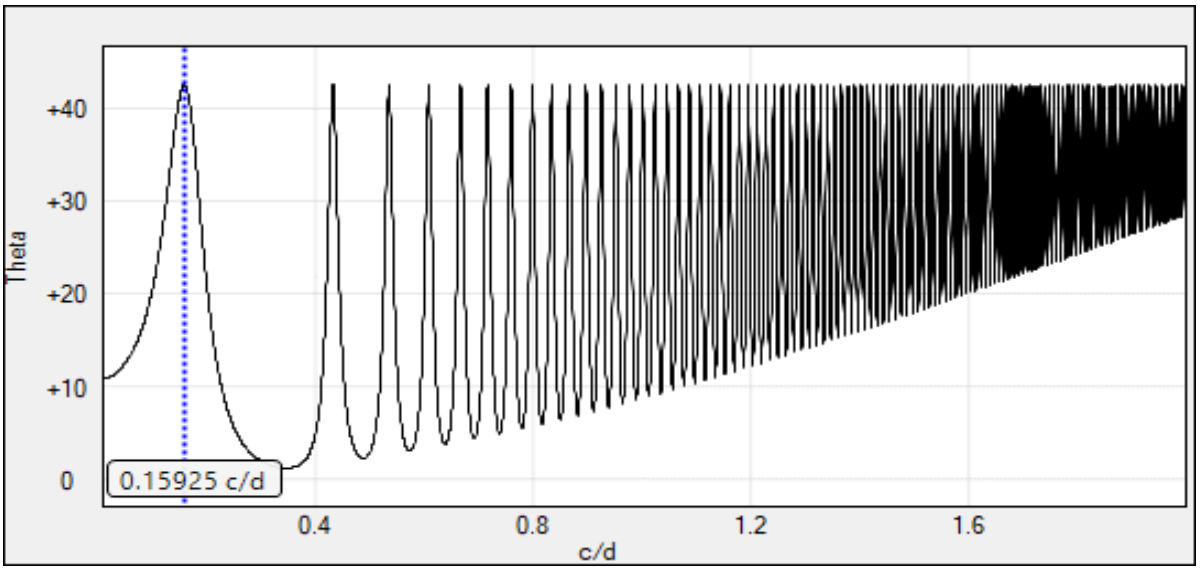

Figure 50: Lomb-Scargle periodogram using PERANSO software for HD 209458 on 2021 September 10-30-10-01

4)

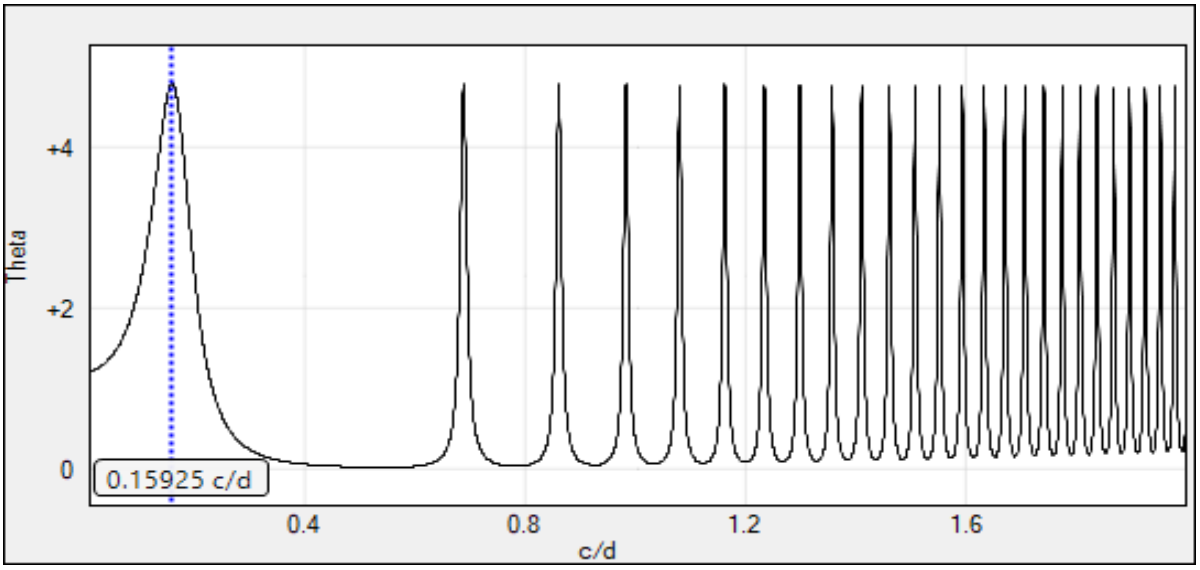

Figure 51: Lomb-Scargle periodogram using PERANSO software for HD 209458 on 2021 October 07-08

5)

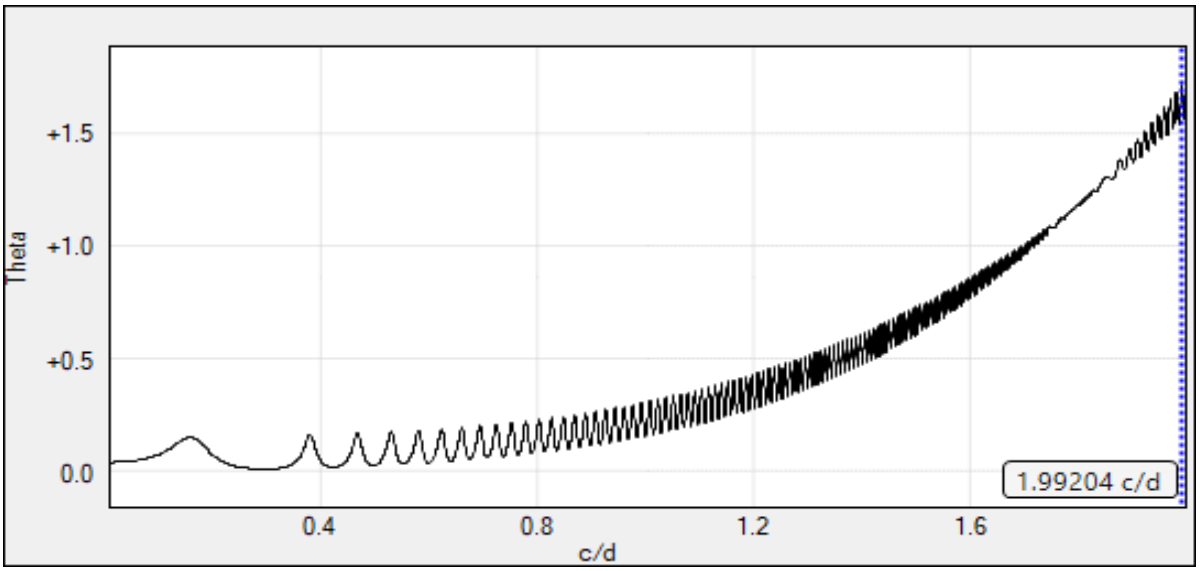

Figure 52: Lomb-Scargle periodogram using PERANSO software for HD 209458 on 2021 October 09-10

6)

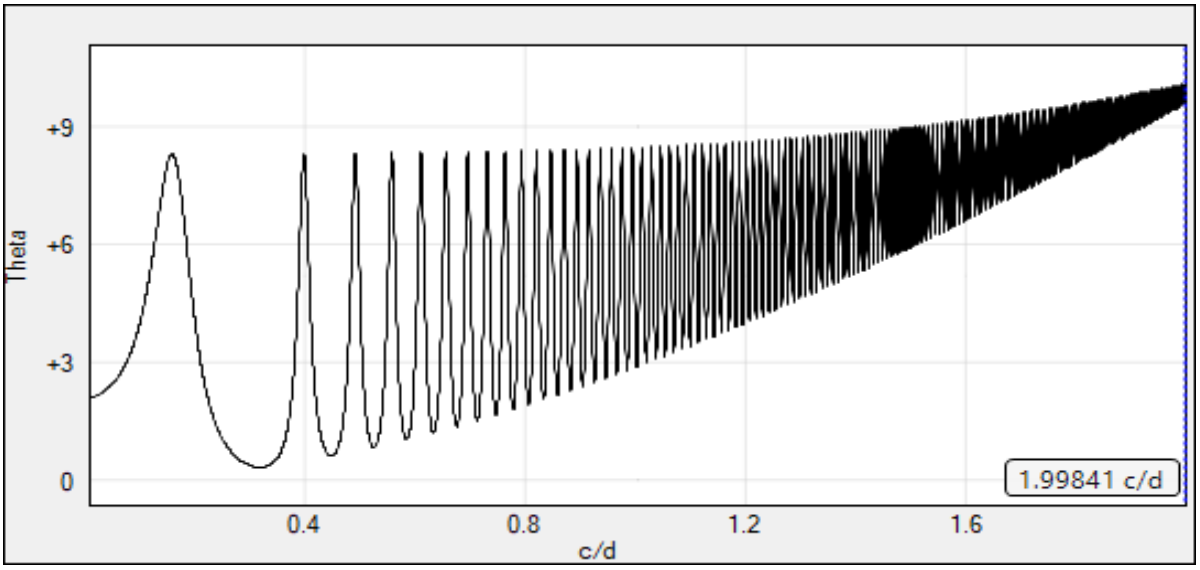

Figure 53: Lomb-Scargle periodogram using PERANSO software for HD 209458 on 2021 October 10-11

7)

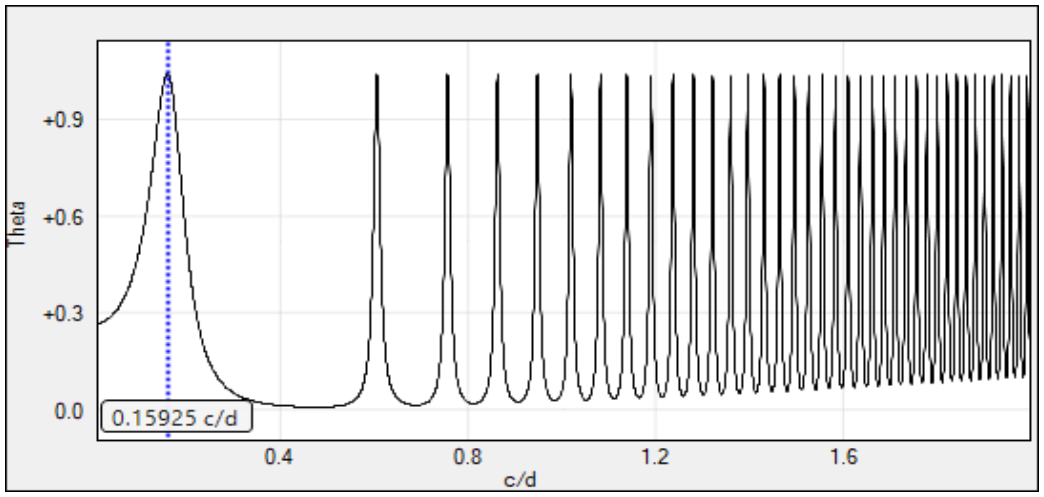

Figure 54: Lomb-Scargle periodogram using PERANSO software for HD 209458 on 2021 October 13-14

8)

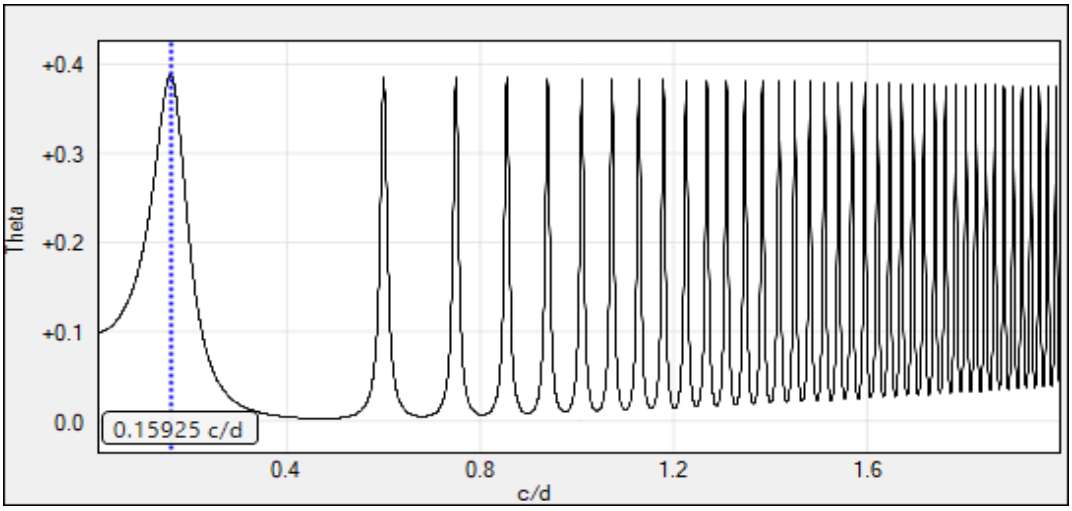

Figure 55: Lomb-Scargle periodogram using PERANSO software for HD 209458 on 2021 October 14-15

As the periodogram analysis shows, the dates September 30 to October 1, October 07-08, October 13-14, October 14-15 all show periods of 0.15925 cycles per day which if converted to days is 6.28 days. That is close to the periodicity of 7 days for HD209458 (Brown et al. 2001), which means that this method does work but if better equipment is used and more stars with SPMI are studies we can verify how well this method works to detect SPMI.

3.14 ANALYSIS OF S FORNACIS USING PERANSO

b) Light Curves for S Fornacis using PERANSO:

1)

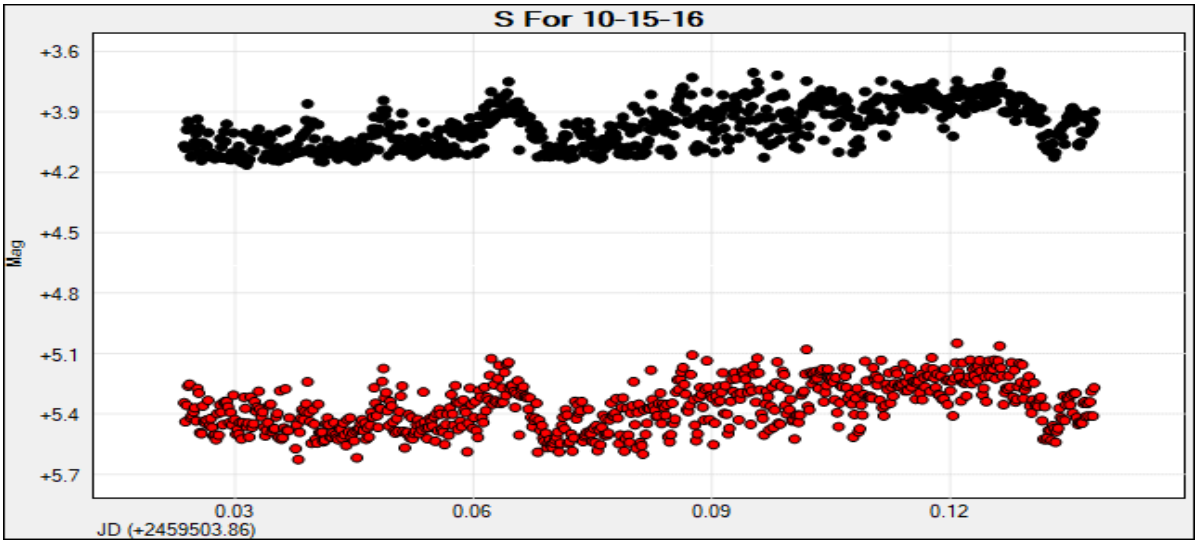

Figure 56: Light curves using PERANSO software for S Fornacis on 2021 October 15-16

2)

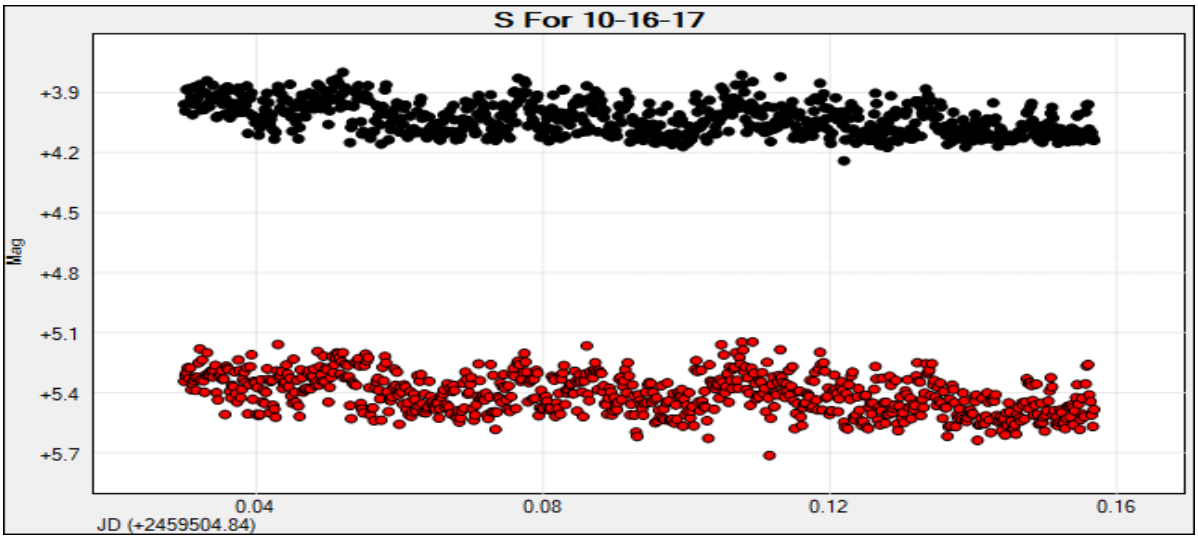

Figure 57: Light curves using PERANSO software for S Fornacis on 2021 October 16-17

3)

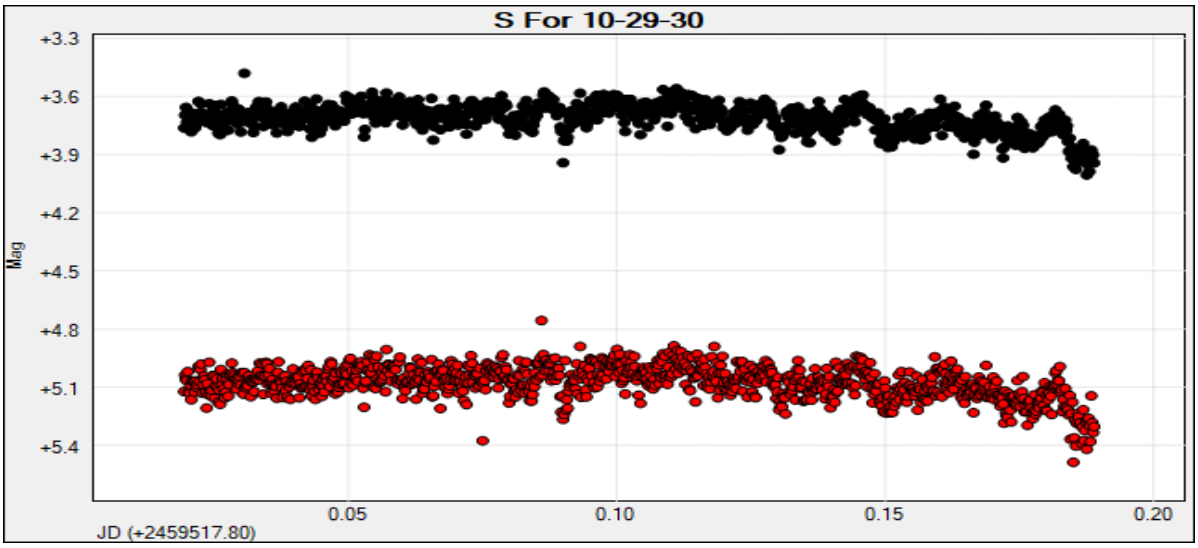

Figure 58: Light curves using PERANSO software for S Fornacis on 2021 October 29-30

4)

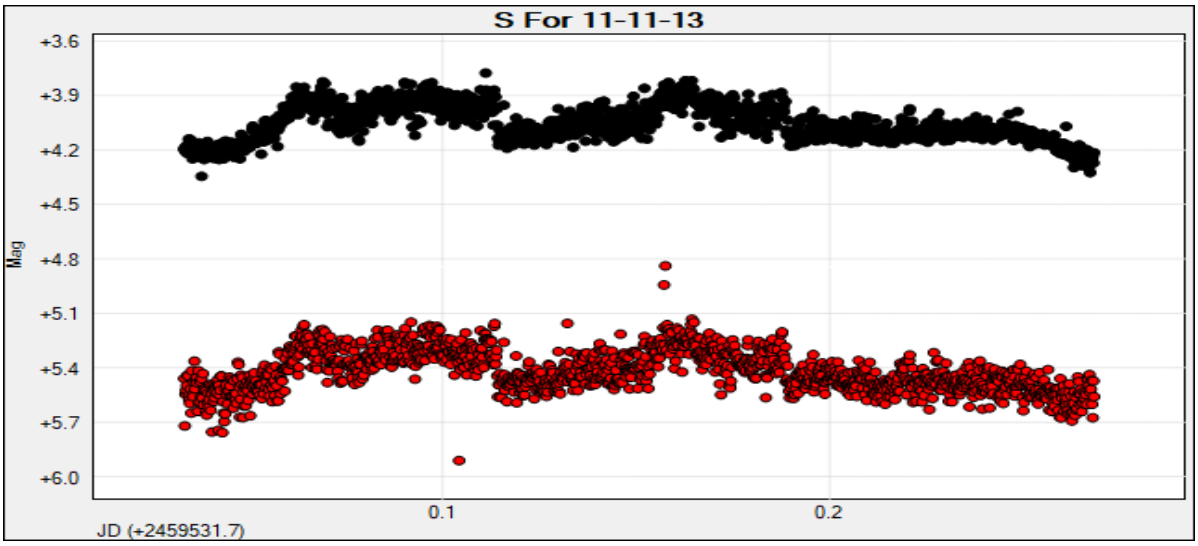

Figure 59: Light curves using PERANSO software for S Fornacis on 2021 November 12-13

5)

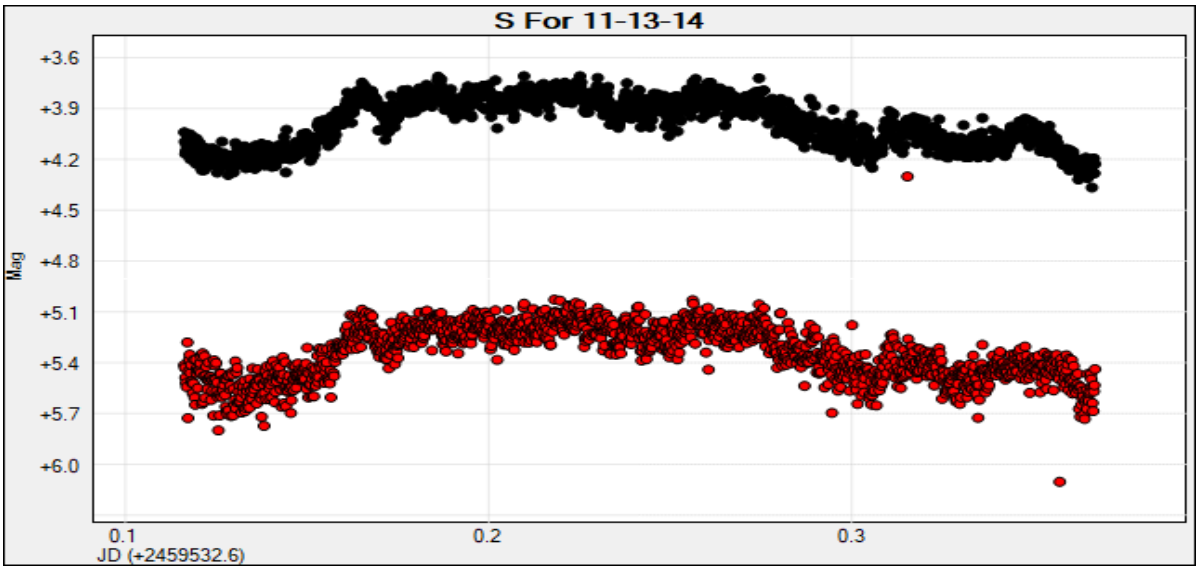

Figure 60: Light curves using PERANSO software for S Fornacis on 2021 November 13-14

6)

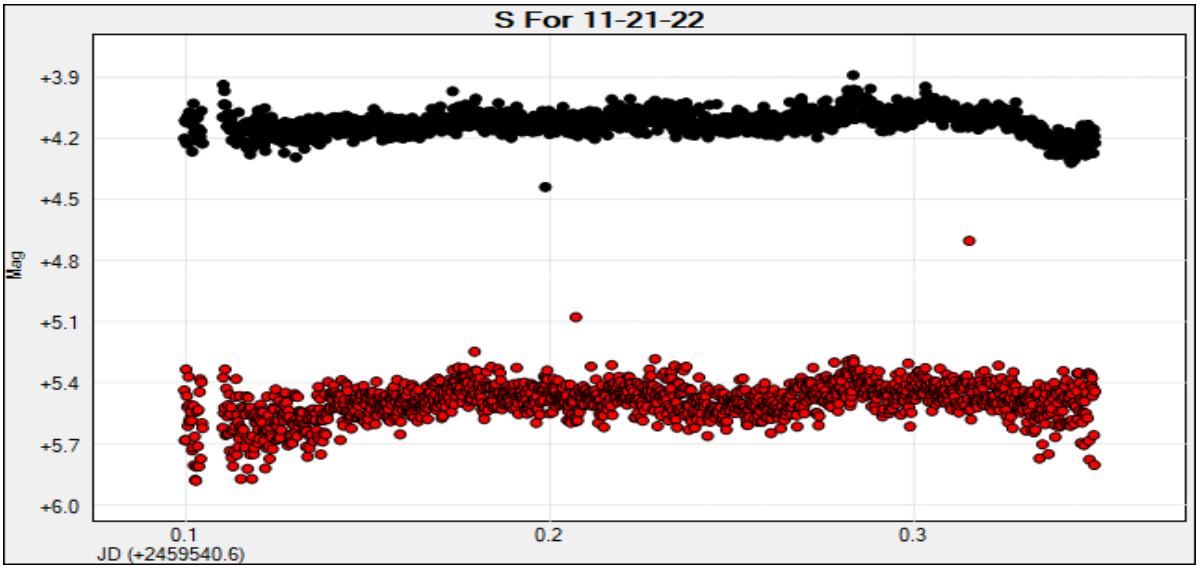

Figure 61: Light curves using PERANSO software for S Fornacis on 2021 November 21-22

After subjecting the time-resolved differential photometry data to light curve analysis in the PERANSO software, it is apparent that no variability is detected through this method in S Fornacis.

3.15 LOMB-SCARGLE PERIODOGRAM ANALYSIS FOR S FORNACIS BETWEEN 1-200 CYCLES/DAY:

1)

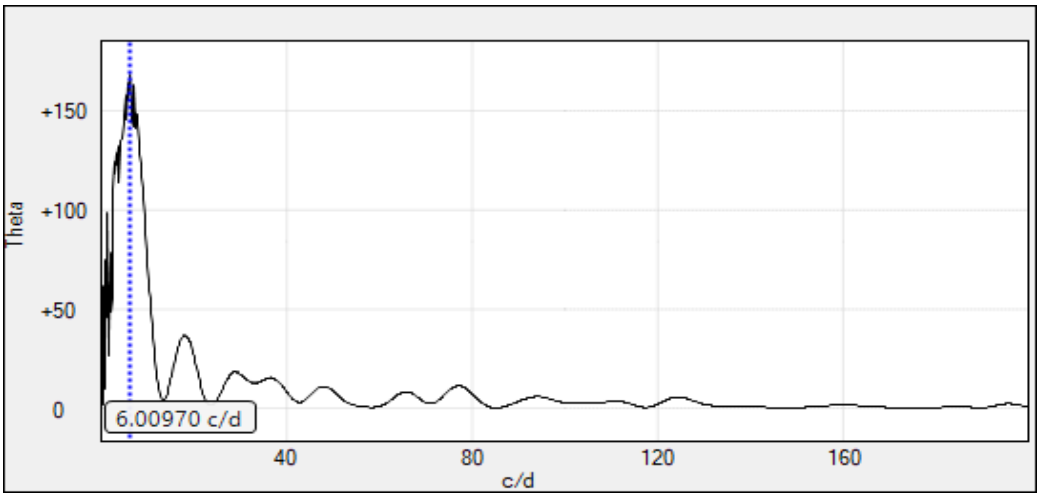

Figure 62: Lomb-Scargle periodogram using PERANSO software for S Fornacis on 2021 October 15-16

2)

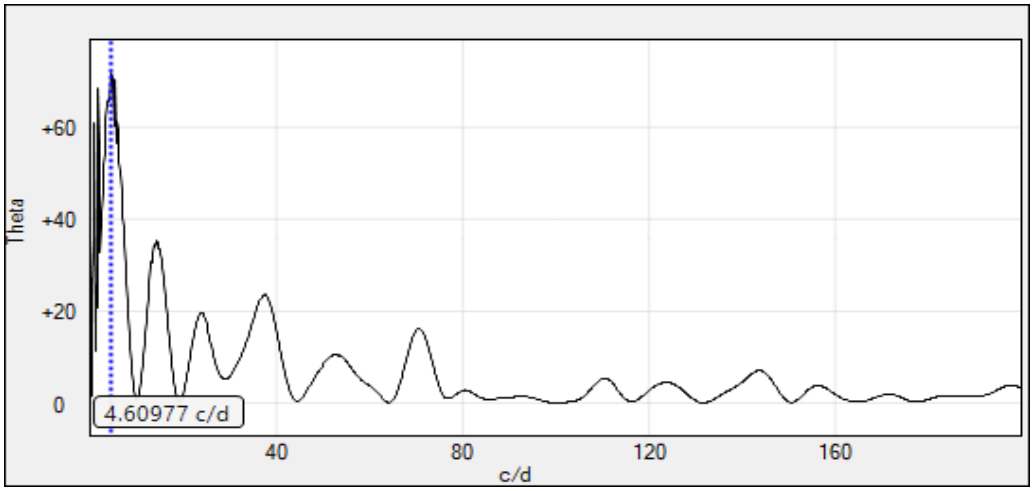

Figure 63: Lomb-Scargle periodogram using PERANSO software for S Fornacis on 2021 October 16-17

3)

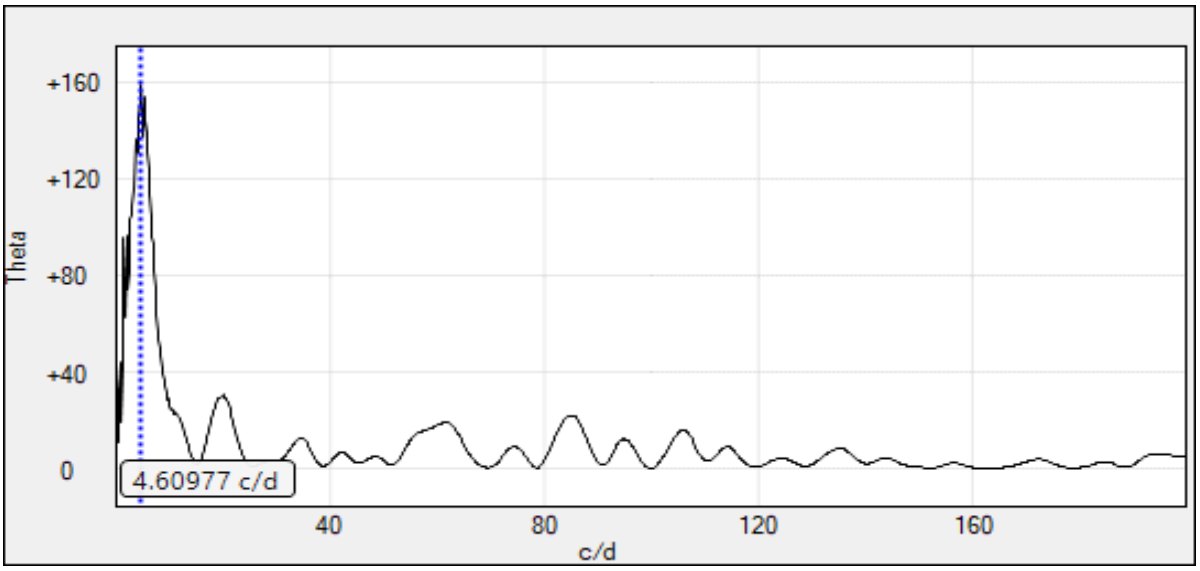

Figure 64: Lomb-Scargle periodogram using PERANSO software for S Fornacis on 2021 October 29-30

4)

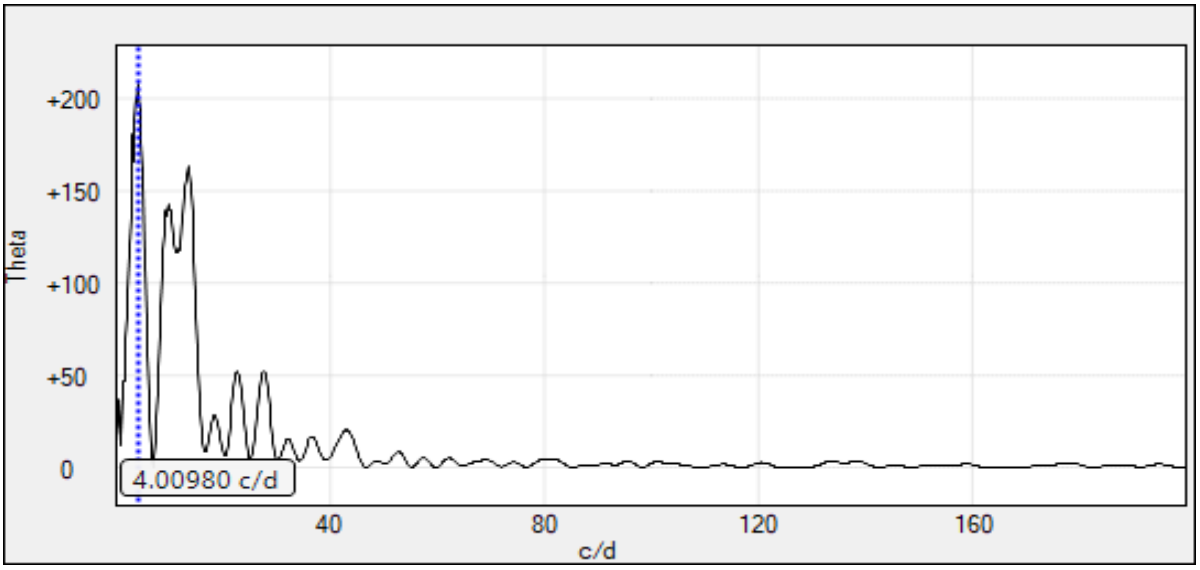

Figure 65: Lomb-Scargle periodogram using PERANSO software for S Fornacis on 2021 November 12-13

5)

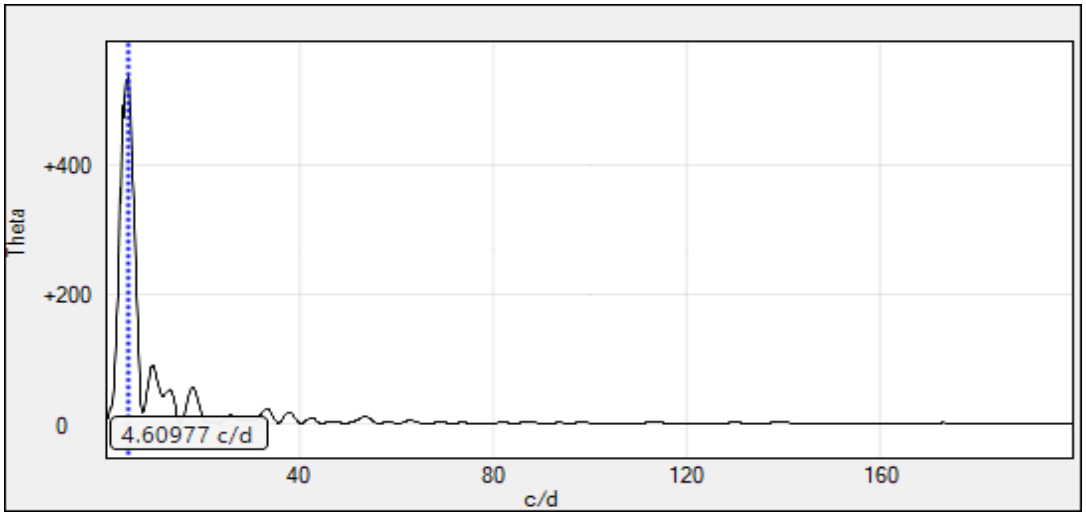

Figure 66: Lomb-Scargle periodogram using PERANSO software for S Fornacis on 2021 November 13-14

6)

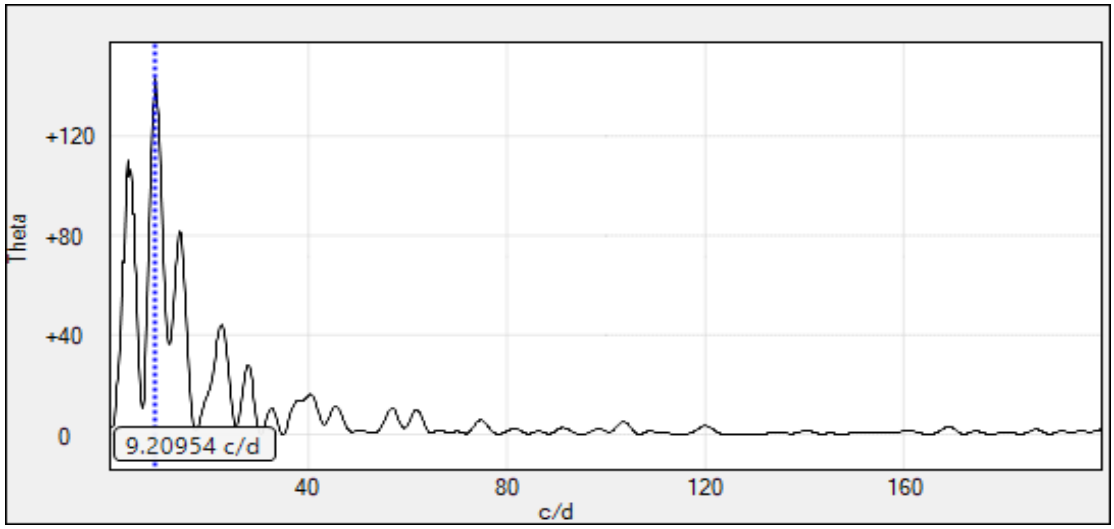

Figure 67: Lomb-Scargle periodogram using PERANSO software for S Fornacis on 2021 November 21-22

Based on the periodogram analysis, most of the periodograms show variability with a periodicity around 4 to 4.6 cycles/day, which corresponds to 6 hours to 5.22 hours respectively. This can be an indication of the variability in the magnitude of S Fornacis.

4. SUMMARY

After looking at the data from Lomb-Scargle periodograms for S Fornacis, we found a regular cycle of 4.60977 times per day in three of the observations, which equals a period of 5.21 hours. Also, for HD 209458, we found a cycle of 0.15925 times per day across four days of observation, which turns out to be 6 days and 6.6 hours.

Now, it's well known that HD 209458 has a transit period of 3.52 days (Brown et al. 2001). But, we are seeing a period of 6 days and 6.6 hours. We think this longer period could be because of magnetic spots. These spots are caused by the interaction between HD 209458 and its passing planet, and they appear and disappear when we look through a special filter (Ca K filter). This may be why we're seeing the period of 6 days and 6.6 hours.

This is the first time we've analyzed variability in S Fornacis like this. The period of 5.21 hours we observed in S Fornacis might also be showing us this kind of interaction between the star and its planet, similar to what we think is happening with HD 209458.As previously mentioned, this thesis aimed to use fractional amount of money to detect SPMI. Our analysis suggest that the light curves plotted using the Time-Resolved Differential Photometry do not display any variability. On the other hand, the periodogram analysis performed on this data, shows promising results of periodicity in both HD209458 and S Fornacis.

While the results from the periodogram analysis are promising, it's important to be cautious. A big concern is the signal-to-noise ratio, which is not at a good level right

now. The noise in the data can hide or change the true signals, which could lead to wrong conclusions. Lowering this ratio is crucial to get the real signals from the data, and thus, make the findings more accurate and reliable.

The way to improve the signal-to-noise ratio is by using better quality astronomical equipment. Investing in expensive telescopes and better spectrographs is a needed step to get clearer observations. These better tools are expected to greatly lower the interference from noise, allowing for a more accurate view of the periodicity seen in HD209458 and S Fornacis. With such improved tools, the journey to confirm the promising results from the periodogram analysis could move forward, making way for more solid and trustworthy findings in the near future.

5. REFERENCES (WORKS CITED, OR SELECTED BIBLIOGRAPHY)

AstroBackyard (2020). Types of Stars | Stellar Classification, Lifecycle, and Charts. Retrieved from https://astrobackyard.com/

Azo Quantum (2023). Hertzsprung-Russell Diagram to Study the Evolutionary Stages of Stars. Retrieved from https://www.azoquantum.com/

Bais, A. F., McKenzie, R. L., Bernhard, G., Aucamp, P. J., Ilyas, M., Madronich, S., & Tourpali, K. (2015). Photochemical & Photobiological Sciences : Official Journal of the European Photochemistry Association and the European Society for Photobiology, Volume 14, Issue 1, pp. 19–52, "Ozone depletion and climate change: impacts on UV radiation" (https://doi.org/10.1039/c4pp90032d)

Berry R. and Burnell J. (2000). The Handbook of Astronomical Image Processing (Willmann-Bell)

Big Think (2021). Hertzsprung-Russell diagram: the most important graph in astrophysics. Retrieved from https://bigthink.com/ (Updated July 15).

Bitner, M.A., Robinson, E. L., & Behr, B.B. (2007). The Astrophysical Journal, Volume 662, Issue 1, pp. 564-573, "The Masses and Evolutionary State of the Stars in the Dwarf Nova SS Cygni"

Brown, T. M., Charbonneau, D., Gilliland, R. L., Noyes, R. W., & Burrows, A. (2001). The Astrophysical Journal, Volume 552, Issue 2, pp. 699–709, "HST Time-Series Photometry of the Transiting Planet of HD 209458"

CESAR - Cosmos (2023). The Hertzsprung-Russell diagram. Retrieved from https://www.cosmos.esa.int/web/cesar/the-hertzsprung-russell-diagram

Cirtain, J.W., Golub, L., Winebarger, A R., de Pontieu, B., Kobayashi, K., Moore, R.L.,Walsh, R.W., Korreck, K.E., Weber, M., McCauley, P., Title, A., Kuzin, S., & Deforest, C.E. (2013). Nature, Volume 493, Issue 7433, pp. 501-503, "Energy release from spatially resolved magnetic braids"

Devorkin, D.H. (1978). Physics Today, Volume 31, Issue 3, pp. 32-39, "Steps toward the Hertzprung–Russell Diagram.

Dineva, E., Pearson, J., Ilyin, I., Verma, M., Diercke, A., Strassmeier, Klaus G., & Denker, C. (2022). Astronomische Nachrichten, Volume 343, Issue 5, article id. e23996, "Characterization of chromospheric activity based on Sun-as-a-star and disk-resolved activity indices"

Dungey, J.W. (1953). Philosophical Magazine, Volume 44, pp. 725-738, “Conditions for the occurrence of electrical discharges in astrophysical systems”

Dungey, J.W. (1961). Physical Review Letters, Volume 6, Issue 2, pp. 47-48, “Interplanetary Magnetic Fields and the Auroral Zones”

Exoplanet Exploration (2021). Stars | What is an Exoplanet? Retrieved from https://exoplanets.nasa.gov/ (Updated April 21)

Giovanelli, F. & Martinez-Pais, I.G. (1991). Space Science Reviews, Volume 56, pp. 313-372, “The cataclysmic variable SS Cygni”.

Giovanelli, R.G. (1948). Monthly Notices of the Royal Astronomical Sociery, Volume 108, pp. 163-176, “Chromospheric flares”

Hesse, M. & Casssak, P.A. (2019). Journal of Geophysical Research: Space Physics, Volume 125, Issue 2, article id. E25935, “Magnetic Reconnection in the Space Sciences: Past, Present, and Future”

Hoyle, F. (1949). Some recent researches in solar physics (Cambridge University Press)

Kitchin, C.R. (2021). Astrophysical Techniques, 7th edition (CRC Press)

Lines, S., Mayne, N. J., Boutle, I. A., Manners, J., Lee, G. K. H., Helling, C., Drummond, B., Amundsen, D. S., Goyal, J., Acreman, D., Tremblin, P., & Kerslake, M. (2018). Astronomy & Astrophysics, Volume 615, id.A97, 23 pp.,“Simulating the cloudy atmospheres of HD 209458 b and HD 189733 b with the 3D Met Office Unified Model.”

Miller-Jones, J.C.A., Sivakoff, G.R., Knigge, C., Körding, E.G., Templeton, M., & Waagen, E.O. (2013). Science, Volume 340, Issue 6135, pp. 950-952, “An Accurate Geometric Distance to the Compact Binary SS Cygni Vindicates Accretion Disc Theory”

Newman, P. (2020). NASA's Imagine the Universe, “Timing and Light Curves.” Retrieved from https://imagine.gsfc.nasa.gov/science/toolbox/timing1.html

Physics LibreTexts (2023). 18.4: The H-R Diagram. Retrieved from https://phys.libretexts.org/ (Updated October 13)

Pillitteri, I. (2019). Star planet magnetic interaction. Retrieved from https://sketchfab.com/3d-models/star-planet-magnetic-interaction-71a173d76fc6419a8965ba2580784a27

Press, W.H., & Rybicki, G.B. (1989). The Astrophysical Journal, Volume 338, pp. 277-280, “Fast Algorithm for Spectral Analysis of Unevenly Sampled Data”

Priest, E. & Forbes, T. (2000). Magnetic Reconnection: MHD Theory and Applications (Cambridge University Press)

Rix, E., et al. (2015). The Patrick Moore Practical Astronomy Series, pp. 249–263, “Calcium K Filters.” https://doi.org/10.1007/978-1-4939-2901-6_6. Accessed 10 May 2023.

Rubenstein, E.P. (2001). American Scientist, Volume 89, Issue 1, pp.38-45, “Superflares and Giant Planets”

Schaefer, B.E., King, J.R., & Deliyannis, C.P. (2000). The Astrophysical Journal, Volume 529, pp. 1026-1030, “Superflares in Ordinary Solar-Type Stars”

Shkolnik, E., Walker, G.A.H., & Bohlender D.A. (2003). The Astrophysical Journal, Volume 597, Issue 2, pp. 1092-1096 “Evidence for Planet-induced Chromospheric Activity on HD 179949”

Shkolnik, E., Walker, G.A.H., Bohlender, D. A., Gu, P.–G., Kürster, M. (2005). The Astrophysical Journal, Volume 622, Issue 2, pp. 1075-1090, “Hot Jupiters and Hot Spots: The Short- and Long-Term Chromospheric Activity on Stars with Giant Planets”

Shkolnik, E., Bohlender, D.A., Walker, G.A.H., & Collier Cameron, A. (2008). The Astrophysical Journal, Volume 676, Issue 1, pp. 628-638, “The On/Off Nature of Star-Planet Interactions”

Sierra Remote Observatories (2023). Retrieved from http://www.sierra-remote.com

Statistics How To. (2023). Residual Plot: Definition and Examples. Retrieved from https://www.statisticshowto.com/residual-plot/

Strugarek, Antoine. (2021). eprint arXiv:2104.05968, “Physics of Star-Planet Magnetic Interactions.” Accessed 10 May 2023.

Universe Today. (2023a). Hertzsprung-Russell diagram. Retrieved from https://www.universetoday.com/39974/hertzsprung-russell-diagram/

Universe Today. (2023b). The Sun. Retrieved from https://www.universetoday.com/16338/the-sun/

VanderPlas, J.T. (2018). The Astrophysical Journal Supplement Series, Volume 236, Issue 1, article id. 16, 28 pp., “Understanding the Lomb–Scargle Periodogram”

Walker, K. (2022). www.bbc.com, 21 Mar. 2022, www.bbc.com/future/article/20220321-what-happened-to-the-worlds-ozone-hole#:~:text=But%20there, “What Happened to the World’s Ozone Hole?” Accessed 10 May 2023.